

# From Deterioration to Acceleration: A Calibration Approach to Rehabilitating Step Asynchronism in Federated Optimization

Feijie Wu, Song Guo, *Fellow, IEEE*, Haozhao Wang, Haobo Zhang, Zhihao Qu, *Member, IEEE*, Jie Zhang, *Member, IEEE*, Ziming Liu

**Abstract**—In the setting of federated optimization, where a global model is aggregated periodically, step asynchronism occurs when participants conduct model training by efficiently utilizing their computational resources. It is well acknowledged that step asynchronism leads to objective inconsistency under non-i.i.d. data, which degrades the model’s accuracy. To address this issue, we propose a new algorithm *FedaGrac*, which calibrates the local direction to a predictive global orientation. Taking advantage of the estimated orientation, we guarantee that the aggregated model does not excessively deviate from the global optimum while fully utilizing the local updates of faster nodes. We theoretically prove that *FedaGrac* holds an improved order of convergence rate than the state-of-the-art approaches and eliminates the negative effect of step asynchronism. Empirical results show that our algorithm accelerates the training and enhances the final accuracy.

**Index Terms**—Federated Learning, Data Heterogeneity, Computational Heterogeneity

## 1 INTRODUCTION

FEDERATED learning (FL) is thriving as a promising paradigm that refrains the leakage of users’ data, including raw information and labels distribution. With the rapid development of FL techniques over the past few years, a wide range of applications for computer vision [1], [2] and natural language processing [3], [4], [5] have deployed over a large set of edge devices (e.g., smartphones and tablets). Conventionally, clients perform a fixed number of local stochastic gradient descent (SGD) steps in each round; then, the server aggregates the updated models and finally acquires and distributes the global one to all clients [6], [7]. FedAvg follows the preceding procedure and has been proven to be a promising solution to data heterogeneity.

With an increasing number of nodes participating in the training, the traditional framework becomes infeasible because the computation capacities are substantially diverse among devices [8]. A practical framework allows clients to update the local model via a flexible number of local SGD steps in each round according to its available resource capacity. And we define such a procedure as *step asynchronism* (see Figure 1 for visualized demonstration). To comprehensively understand the training performance of the traditional algo-

TABLE 1: The number of communication rounds to reach the test accuracy of 80% under Logistic Regression (LR) and 2-layer CNN on Fashion-MNIST with various settings when 10 devices participate in FedAvg. The number of local updates is 100 without step asynchronism, while under step asynchronism, clients perform at least 100 local updates. The learning rates set for LR and 2-layer CNN are 0.001 and 0.03, respectively, which are also applied to Table 2, Figure 2, and Figure 3.

FedAvg with	LR	2-layer CNN
neither	2	20
step async	1	8
non-i.i.d.	91	265
both	1K+	339

gorithm FedAvg, Table 1 compares the results in terms of test accuracy in two situations – step asynchronism and data heterogeneity. This experiment is under convex (i.e., logistic regression) and non-convex (i.e., 2-layer CNN) objectives using a public dataset Fashion-MNIST [9]. Performance deterioration is noticeable, especially in the logistic regression model the desired test accuracy cannot be reached.

A previous study [10] owes the performance deterioration to *objective inconsistency*, where the FL training converges to a stationary point that mismatches the optimal solution. In order to alleviate the issue, Wang et al. [10] introduce FedNova, a normalization approach that averages the normalized local gradients and accordingly updates the global model at the server. However, in Table 2, we empirically disclose that FedNova cannot fully utilize the computational resources of the powerful node under heterogeneous environments, which explicitly limits the number

- Song Guo and Zhihao Qu are the corresponding authors.
- Feijie Wu, Song Guo, Jie Zhang and Ziming Liu are with the Department of Computing, The Hong Kong Polytechnic University, Hong Kong (email: {harli.wu, jieaa.zhang, ziming.liu}@connect.polyu.hk, song.guo@polyu.edu.hk)
- Haozhao Wang is with the School of Computer Science and Technology, Huazhong University of Science and Technology, Wuhan, China (e-mail: hz\_wang@hust.edu.cn).
- Haobo Zhang is with Computer Science and Engineering department, Michigan State University, East Lansing, MI, USA (email: zhan2060@msu.edu).
- Zhihao Qu is with the School of Computer and Information, Hohai University, Nanjing, China (e-mail: quzhihao@hhu.edu.cn).

TABLE 2: Utilization and test accuracy under the setting that one Nvidia GTX 3080Ti and nine other devices are shown in the first column. Here we evaluate Fashion-MNIST with non-convex objectives (i.e., 2-layer CNN), and the data distribution among clients is heterogeneous.

Device	Method	Utilization <sup>1</sup> (Rounds)	Accuracy(%) <sup>2</sup>
Raspberry Pi 4	FedNova	25% (49)	66.18
	FedaGrac	<b>100% (25)</b>	<b>72.07</b>
Nvidia Jetson Nano	FedNova	50% (50)	64.39
	FedaGrac	<b>100% (21)</b>	<b>72.93</b>
Nvidia GTX 1080 Ti	FedNova	100% (40)	69.77
	FedaGrac	<b>100% (30)</b>	<b>72.00</b>
Nvidia GTX 2080 Ti	FedNova	100% (29)	72.11
	FedaGrac	100% (36)	<b>72.13</b>

<sup>1</sup>Utilization means the maximum computation capacity of Nvidia GTX 3080Ti to achieve the test accuracy of 60% in the first 50 rounds. We obtain the value by tuning the resource usage from 100% and looping a deduction of 5%. Rounds quantify when the approach achieves 60% test accuracy.

<sup>2</sup>Given the utilization, we measure the test accuracy after 100 rounds.

of local updates for the faster node.

In this paper, we propose a method named `FedaGrac` to conquer the objective inconsistency challenge under a highly imbalanced computational setting in FL. The core idea of our proposed algorithm is to calibrate each local update according to the global update orientation. Although the correct global direction is not known, it can be estimated based on the clients’ local updates: If a client performs the local updates very fast, then the client will transmit the first gradient; otherwise, the averaged gradient. By this means, the negative effect of deviation on the convergence can be significantly mitigated. We conduct preliminary experiments and depict the comparison between our proposed algorithm and FedNova [10] in terms of resource utilization and test accuracy in Table 2. In all cases, `FedaGrac` not only fully utilizes the computational resources, but also achieves a better accuracy than FedNova (see Table 2).

Our key contributions to this work are listed as follows:

- 1) To explore the factors that lead to performance deterioration, we analyze the convergence property under strongly-convex objectives. The theoretical result indicates that the expected loss never reaches the optimal one when both data heterogeneity and step asynchronism exist. In other words, a constant number of local updates eliminates the negative effect of data distribution differentiation, while step asynchronism magnifies the drawback of data heterogeneity.
- 2) We design a novel method named `FedaGrac` to address the problem of objective inconsistency via predictive gradient calibration, which makes the direction of each local update close to the direction towards the global optimum. For the first time, our algorithm can jointly address statistical heterogeneity and computation heterogeneity at a time.
- 3) We establish the convergence rate of `FedaGrac`. Under non-convex objectives, the algorithm achieves a convergence rate of  $O\left(1/\sqrt{MT\bar{K}}\right)$ , where  $M$

and  $T$  represent the number of clients and communication rounds, respectively, and  $\bar{K}$  indicates the weighted averaged number of local updates. This convergence rate is also achieved by FedNova only under the condition that  $K_{\max}/K_{\min} = O(M)$ , where  $K_{\max}$  and  $K_{\min}$  separately refer to the maximum and minimum number of local updates [10]. Otherwise, the actual convergence rate of FedNova should be  $O\left(\sqrt{\bar{K}/MT}\right)$ . Apparently, our algorithm can achieve a faster convergence rate by a factor up to  $O(\bar{K})$ .

- 4) We conduct extensive experiments to compare the proposed `FedaGrac` with typical and latest works such as SCAFFOLD [11] and FedNova [10]. In terms of convergence rate, `FedaGrac` achieves higher convergence efficiency compared to FedAvg and FedNova, especially in scenarios with high heterogeneity. For example, in terms of test accuracy, our algorithm can always preserve convergence while SCAFFOLD and FedNova cannot in some cases.

The rest of this paper is organized as follows. First, Section 2 provides related work and background knowledge of distributed SGD and existing solutions to heterogeneous training. Next, we state preliminaries and problem formulation for the heterogeneous Federated Learning in Section 3. Then, in Section 4, we design a novel algorithm `FedaGrac` to solve the problem. In Section 5, we analyze its convergence property. After that, we present our experimental results to evaluate our method in Section 6. Finally, Section 7 concludes the paper.

## 2 RELATED WORK

**Federated learning.** Frequently, edge devices such as smartphones possess abundant data, which are highly sensitive but useful to the model training [12], [13], [14], [15]. To utilize these data, FL is conceived to search for a generalized model [16], [17], [18] or personalized models [19], [20], [21] while safeguarding the data privacy [6], [22]. Apparently, the data are heterogeneous among clients because there are no predefined rules for the data distribution for each client. Besides, due to the hardware differences among devices, the computational capabilities are various. In this section, we briefly investigate the flaws raised by data heterogeneity and computation heterogeneity and review the existing work to tackle these two issues.

**Data Heterogeneity.** Generally, in FL settings, the data distributed among clients are agnostic and therefore, each data portfolio has its exclusive optimal parameters. As a classical algorithm to combat data heterogeneity, FedAvg inherits the training features from local SGD [23], [24], [25], a framework that runs for multiple local updates prior to a global synchronization. Obviously, this strategy significantly reduces the total communication overhead when compared to parallel SGD that synchronizes the gradient at every local update. Recent studies [7], [26], [27] show that FedAvg can have a great performance from theoretical and empirical perspectives. Also, FedAvg can seamlessly adopt communication-efficient approaches such as quantization

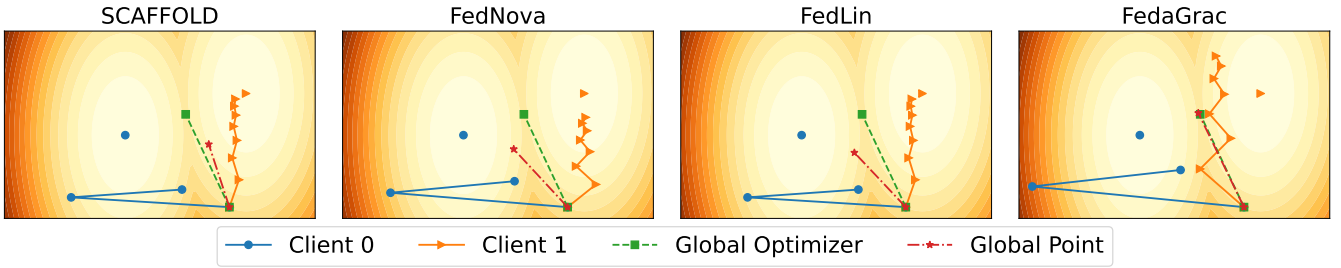


Fig. 1: Illustration of model updating in the parameter space. For client  $i$ , we generate a set of  $(x, y)$ s fluctuated around a linear function  $y = a_i x + b_i$ , where  $a_i$  and  $b_i$  are real numbers. Our target is to find an optimal straight line  $y = ax + b$ , which is averagely close to all clients' data. Starting at the same point, each client applies mean squared error (MSE) loss and follows a predefined algorithm to update its local model so as to optimize the global one. Regarding the existence of data and computation heterogeneity, our proposed method does not deviate from the direction towards a global minimizer.

[28], [29], [30] and sparsification [31], [32] to further reduce the cost of transmission [33], [34], [35], [36].

Nevertheless, numerous studies [11], [37], [38], [39], [40] theoretically prove that the issue raises the client-drift effect and degrades the convergence property. To mitigate the negative impact, existing solutions include cross-client variance reduction [11], [41], client clustering sampling [42], [43], [44] and reinforcement learning driven incentive mechanism [45]. Among these approaches, SCAFFOLD [11] is a superior option that adjusts every local update with the help of the global and a client's local reference orientation, such that every local update keeps close to the global direction. However, as shown in Figure 1, SCAFFOLD cannot completely remove the drift. A physical explanation for the result is that the local reference directions of the faster nodes with more number of local updates lead to a significant deviation from the orientation towards the local optimizer. Since the global reference direction is aggregated by clients' local ones, it is intuitively dominated by the faster nodes (see Figure 1), which betrays its origin intention. Although we use a similar design philosophy that ensures every local update along with the global orientation, the global orientation consists of the gradient that depends on the number of local updates, either the normalized gradient or the initial gradient.

**Computational Heterogeneity.** The computation capabilities vary among clients because they use different devices. To minimize the computation differences, some existing works adopt a client sampling strategy [46], [47], [48], [49], where only a small portion of clients transmit the gradients to the server. Compared to the case that requires full-worker participation, this scheme reduces the total training time. However, there still exists resource underutilization as the fastest client should wait for others' completion.

A practical solution is to adopt step asynchronism, where each client performs an inconsistent number of local updates. Although FedAvg with step asynchronism can converge to a stable point under non-convex objectives [24], Wang et al. [10] point out that objective inconsistency takes place under quadratic function. To alleviate the challenge of computational heterogeneity, effective approaches are constituted with normalization-based approach FedNova [10] and FedLin [50], regularization-based approach Fed-Prox [51] and architecture-based approach HeteroFL [52].

Gradient normalization is the most ubiquitous framework that overcomes step asynchronism under non-i.i.d. data setting. However, this method cannot prevent the negative impact of statistical heterogeneity on the convergence rate because the update deviation still exists after averaging. Figure 1 compares FedNova [10] and FedLin [50] with our proposed method, and we notice that the global model deviates to the one with less updates in FedNova [10]. The reason is obvious: clients update the models bias to their local datasets such that the normalized gradients collected by the server are sparse. Besides, with the local models approaching the local minimizers, the update becomes so trivial that those clients with more local updates have a dispensable influence on the global model update.

### 3 PRELIMINARY AND PROBLEM FORMULATION

Formally, the learning problem can be represented as the following distributed optimization problem across  $M$  FL clients:

$$\min_{\mathbf{x} \in \mathbb{R}^d} F(\mathbf{x}) = \sum_{i=1}^M \omega_i F_i(\mathbf{x}), \quad (1)$$

where the weight  $\omega_i = |\mathcal{D}_i|/|\mathcal{D}|$  is the ratio between the size of local dataset  $\mathcal{D}_i$  and overall dataset  $\mathcal{D} \triangleq \cup_{i=1}^M \mathcal{D}_i$ , and  $F_i(\mathbf{x}) \triangleq \mathbb{E}_{\varepsilon_i \sim \mathcal{D}_i} [f_i(\mathbf{x}; \varepsilon_i)]$  is the local objective, i.e., the expected loss value of model  $x$  with respect to random sampling  $\varepsilon_i$  for client  $i$ .

**FedAvg with step asynchronism.** Naive weighted aggregation [6], [23], [7], [24] is an effective and communication-efficient way to solve Problem (1) for both convex and non-convex objectives. With the increasing number of edge devices participating in model training, the framework is neither economic nor fair to require all clients to run a certain number of local updates. Instead, a practical approach is that client  $i \in \{1, \dots, M\}$  runs for a flexible number of SGD steps (i.e.,  $K_i$ ) according to its resource capability before the model aggregation at the server:

- **(Pull):** Pulls the current parameter  $\mathbf{x}_0$  from the server.
- **(Compute):** Samples a realization  $\varepsilon$  randomly from the local dataset  $\mathcal{D}_i$  and compute the gradient  $\nabla f_i(\mathbf{x}_k, \varepsilon)$ .

- **(Update):** Performs  $k$ -th local update of the form  $\eta$  by  $\mathbf{x}_{k+1} = \mathbf{x}_k - \eta \mathbf{g}_k$ , where  $k \in \{0, \dots, K_i\}$  and  $\eta$  is the stepsize.
- **(Push):** Pushes the local parameter  $\mathbf{x}_{K_i}$  to the server.

Under this framework, we let  $K_{\max}$  and  $K_{\min}$  separately be the maximum and the minimum number of local updates among all clients, i.e.,  $K_{\max} = \max_{i \in \{1, \dots, M\}} K_i$  and  $K_{\min} = \min_{i \in \{1, \dots, M\}} K_i$ . In addition,  $\bar{K} = \sum_{i=1}^M \omega_i K_i$  is defined as the weighted averaged number of local updates. Formally, step asynchronism is defined as the following mathematical expression:

$$\exists i, j \in \{1, \dots, M\}, \quad K_i \neq K_j. \quad (2)$$

Therefore,  $K_{\max} \neq K_{\min}$  when step asynchronism exists. Without extra explanations, these notations are adopted throughout the paper.

**Assumptions.** To establish the convergence theory of the FL optimization, we make the following assumptions that are adapted in previous works [7], [10], [53], [51], [54]:

**Assumption 1 (L-smooth).** *The local objective functions are Lipschitz smooth: For all  $v, \bar{v} \in \mathbb{R}^d$ ,*

$$\|\nabla F_i(v) - \nabla F_i(\bar{v})\|_2 \leq L\|v - \bar{v}\|_2, \quad \forall i \in \{1, \dots, M\}.$$

**Assumption 2 ( $\mu$ -strongly convex).** *The local objective functions are  $\mu$ -strongly convex with the value of  $\mu > 0$ : For all  $v, \bar{v} \in \mathbb{R}^d$ ,*

$$F_i(v) - F_i(\bar{v}) \geq \langle \nabla F_i(\bar{v}), (v - \bar{v}) \rangle + \frac{\mu}{2} \|v - \bar{v}\|_2^2, \\ \forall i \in \{1, \dots, M\}$$

where  $\langle \cdot, \cdot \rangle$  refers to the inner product of two gradients.

**Assumption 3 (Bounded Variance).** *For all  $v \in \mathbb{R}^d$ , there exists a scalar  $\sigma \geq 0$  such that*

$$\mathbb{E}\|\nabla f_i(v, \epsilon) - \nabla F_i(v)\|_2^2 \leq \sigma^2, \quad \forall i \in \{1, \dots, M\}$$

**Assumption 4 (Bounded Dissimilarity).** *For some  $v \in \mathbb{R}^d$  that  $\|\nabla F(v)\|_2^2 > 0$  holds, there exists a scalar  $B \geq 1$  such that*

$$\mathbb{E}\|\nabla F_i(v)\|_2^2 \leq B^2 \|\nabla F(v)\|_2^2, \quad \forall i \in \{1, \dots, M\}.$$

Obviously, when the data are independent and identically distributed, the value of  $B$  should be 1.

Assumption 4 seems to be a little bit strong as  $\|\nabla F(v)\|_2^2$  cannot be 0. However, considering  $\epsilon$ -accuracy as the learning criterion, i.e.,  $\|\nabla F(v)\|_2^2 \leq \epsilon$  under non-convex objectives such as deep neural networks which possess multiple local minimizers, the value of  $\epsilon$  cannot strictly be 0. In other words, there exists  $\epsilon_1 \leq \epsilon$  such that  $\|\nabla F(v)\|_2^2 \geq \epsilon_1$  for all  $v$  always holds.

**Key factor that raises objective inconsistency.** Although [10] indicates that objective inconsistency occurs when using FedAvg with step asynchronism under quadratic functions, the factor that makes it happen remains a mystery. To explore in depth, the following theorem analyzes FedAvg with step asynchronism under a strongly-convex objective.

**Theorem 1.** *Suppose the local objective functions are non-negative. Denote the parameter at  $t$ -th communication round by  $\mathbf{x}_t$ . Let  $T$  be the total number of communication rounds. Under Assumption 1, 2, 3 and 4, by setting the learning rate*

$\eta = \mathcal{O}(1/\mu L T \bar{K}) \leq 1/L\bar{K}$ , the output of FedAvg with step asynchronism satisfies

$$\lim_{T \rightarrow \infty} \mathbb{E}[F(\mathbf{x}_T)] - F(\mathbf{x}_*) \leq \mathcal{O} \left( \sum_{i=1}^M \omega_i \left( \frac{K_i}{K_{\min}} - 1 \right) F_i(\mathbf{x}_*) \right) \quad (3)$$

where  $\mathbf{x}_1$  and  $\mathbf{x}_*$  indicates the initial and optimal model parameters, respectively.

*Proof.* See Appendix A for details.  $\square$

**Remark** The theoretical result in Equation 3 is consistent with the result of FedAvg analysis in [11] as the number of local updates is identical, i.e.,  $K_i = \bar{K}, \forall i \in \{1, \dots, M\}$ . Besides, when the data are identical and independent distributed among clients, where the global optimizer is not equivalent to the clients' local minimizer, we can easily induce that  $\mathbf{x}_T$  is close to  $\mathbf{x}_*$  when  $T \rightarrow \infty$ . The conclusion holds regardless of the number of local updates. However, when data heterogeneity and step asynchronism coexist, the right-hand side of Equation (3) is non-zero. As a result, when  $T$  tends to be infinite, the model cannot converge to the optimal parameters, which can explain the result manifested in Table 1 under LR. Based on the theoretical discovery, we can draw a conclusion that step asynchronism leads to a significant accuracy drop in the non-i.i.d. cases, which impedes normal training.

## 4 FEDAGRAC ALGORITHM

To ensure that  $\mathbb{E}[F(\mathbf{x}_T)] - F(\mathbf{x}_*)$  is close to 0 when  $T \rightarrow \infty$ , we target to remove the constant term in the right-hand side of Equation (3). Based on the remark in Section 3, a practical approach is to minimize the effectiveness of data heterogeneity. In this section, we elaborate our proposed algorithm, Federated Accelerating Gradient Calibration (FedAgrac), to avoid the objective inconsistency as well as enhance the convergence performance when step asynchronism is adopted to improve the resource utilization. The implementation details are presented as Algorithm 1.

At first, apart from the hyperparameters such as learning rate  $\eta$  and calibration rate  $\lambda$ , we initialize a  $d$ -dimension model with arbitrary parameters  $\mathbf{x}_1$ . Besides, to ease the theoretical analysis in Section 5, we set  $\nu^{(i)}$  as  $\nabla f_i(\mathbf{x}_1, \mathcal{D}_i)$  for all  $i \in \{1, \dots, M\}$ . Then, we define  $\nu$  as:

$$\nu = \sum_{i=1}^M \omega_i \nu^{(i)} = \sum_{i=1}^M \omega_i \nabla f_i(\mathbf{x}_1, \mathcal{D}_i).$$

In this algorithm, client  $i$  performs the local updates for  $K_i$  times in parallel. During each local update, clients calibrate the local client deviation with reference to the global reference orientation, which is estimated at every global synchronization. In the following two subsections, we separately discuss the effectiveness of two main components, namely,

- **Calibrating the local client deviation** (Line 9 in Algorithm 1) migrates the data heterogeneity;
- **Estimating the global reference orientation** (Line 14 in Algorithm 1) accelerates the training process.

---

**Algorithm 1** Federated Accelerating Gradient Calibration (FedAGrac)
 

---

**Require:** Initialize  $M$  clients, set the initial model to be  $\tilde{\mathbf{x}}_1 \in \mathbb{R}^d$ . Set  $\nu^{(i)}$  and  $\nu$  for all clients  $i \in \{1, \dots, M\}$ . Set learning rate  $\eta > 0$ , calibration rate  $\lambda > 0$ , the number of global synchronizations  $T$  and the number of local iterations of each client  $K_i$  for all clients  $i \in \{1, \dots, M\}$ .

- 1: **On client**  $i \in \{1, \dots, M\}$ :
  - 2: **for**  $t = 1$  to  $T$  **do**
  - 3: Pull  $\tilde{\mathbf{x}}_t, \nu$  from server
  - 4: Set  $\mathbf{x}_{t;0}^{(i)} = \tilde{\mathbf{x}}_t$
  - 5: Set  $\mathbf{c} = \nu - \nu^{(i)}$
  - 6: **for**  $k = 0$  to  $K_i - 1$  **do**
  - 7: Randomly sample a realization  $\varepsilon_k^{(i)}$  from  $\mathcal{D}_i$
  - 8:  $\mathbf{g}_{t;k}^{(i)} = \nabla f_i(\mathbf{x}_{t;k}^{(i)}, \varepsilon_k^{(i)})$
  - 9:  $\mathbf{x}_{t;k+1}^{(i)} = \mathbf{x}_{t;k}^{(i)} - \eta(\mathbf{g}_{t;k}^{(i)} + \lambda \mathbf{c})$
  - 10: **end for**
  - 11: Set  $\nu^{(i)} = \frac{1}{K_i} \sum_{k=0}^{K_i-1} \mathbf{g}_{t;k}^{(i)}$
  - 12: Push  $\mathbf{x}_{t;K_i}^{(i)}, K_i$  to the server
  - 13: Receive  $\bar{K}$  from the server
  - 14: if  $K_i \leq \bar{K}$ , then send  $\nu^{(i)}$ ; else send  $\mathbf{g}_{t;0}^{(i)}$
  - 15: **end for**
  - 16: **On server:**
  - 17: **for**  $t = 1$  to  $T$  **do**
  - 18: Push  $\tilde{\mathbf{x}}_t, \nu$  to clients
  - 19: Pull  $\mathbf{x}_{t;K_i}^{(i)}, K_i$  from client  $i \in [1, \dots, M]$
  - 20:  $\tilde{\mathbf{x}}_{t+1} = \sum_{i=1}^M \omega_i \mathbf{x}_{t;K_i}^{(i)}$
  - 21:  $\bar{K} = \sum_{i=1}^M \omega_i K_i$
  - 22: Push  $\bar{K}$  to clients and receive  $v_{\text{transit}}^{(i)}$  from clients
  - 23:  $\nu = \sum_{i=1}^M \omega_i v_{\text{transit}}^{(i)}$
  - 24: **end for**
- 

#### 4.1 Calibrating the local client deviation

As a classical approach, FedAvg updates the parameters using stochastic gradient descent (SGD), where the gradient is computed in accordance with Line 8. Suppose the gradient is equivalent to the first order derivative of the true local objective, i.e.,  $\nabla f_i(v, \varepsilon) = \nabla F_i(v)$ , where  $\varepsilon$  is randomly sampled from the local dataset  $\mathcal{D}_i$ . Then, given the stepsize  $\eta$ , the model update follows  $\mathbf{x}_{t;k+1}^{(i)} = \mathbf{x}_{t;k}^{(i)} - \eta \nabla F_i(\mathbf{x}_{t;k}^{(i)})$ . Previous works [55], [56] show that this scheme can converge to a stable point when a client performs sufficient local updates. Under a heterogeneous data setting, the points vary among clients because each of them is determined by the local data distribution. Therefore, clients are biased from the global orientation, and the phenomenon is named as client deviation<sup>1</sup>.

Existing works to overcome client deviation mainly focus on the variance reduction approach, i.e., SCAFFOLD [11]. It is somehow similar to our proposed algorithm when  $\lambda$  is set to 1. In this case, client  $i$ 's local reference direction  $v^{(i)}$  is assumed to be equivalent to the vector from the current point to its local optimizer. As for the global reference orientation,  $v$  overlaps with the gradient from the current point to the global minimizer. However, it is

1. Client deviation is also known as client drift [11], [50].

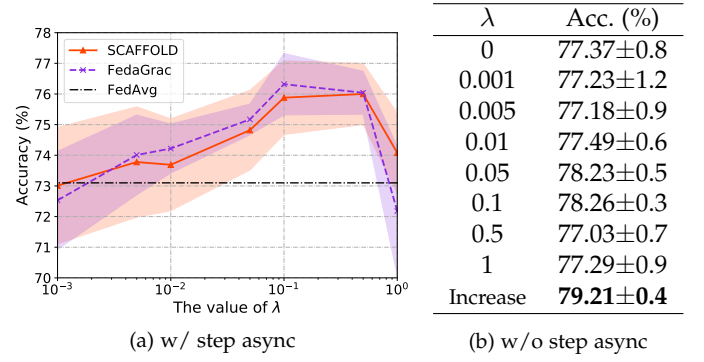


Fig. 2: Preliminary experiments for a 2-layer CNN with the recognition of Fashion-MNIST. In the line graph 2a, the experiments are conducted when the clients perform various numbers of local steps. The vertical axis indicates the test accuracy after 200 rounds, while the horizontal axis shows the value of calibration rate  $\lambda$ . As for the table 2b, clients perform constant local updates. The algorithm is equivalent to FedAvg when  $\lambda = 0$ . “Increase” in the table shows the value of  $\lambda$  changes over time, i.e., 0.1 for the first 50 rounds, 0.5 for the next 100 rounds, and 1 for the rest.

nearly impossible to coincide with the case, especially when applied with the gradient calibration technique. Generally speaking, using an obsolete gradient to predict the coming gradient is not reasonable because the aggregated direction presumably deviates from the expected one.

Therefore, we introduce a calibration rate  $\lambda$  for the correction term. With this hyperparameter, a gradient can be adjusted and approximated to the global update. Empirical results in Figure 2 intuitively present the effectiveness of  $\lambda$ . Generally speaking, a smaller  $\lambda$  has a similar performance as FedAvg because the calibrated gradient is still biased to the local computed one. For a greater  $\lambda$ , the test accuracy goes down dramatically since the gradient is over-calibrated. As a result, a constant  $\lambda$  cannot be too large or too small such that the calibration term is effective. Furthermore, in Figure 2b, we evaluate a case where  $\lambda$  increases over time. Apparently, the strategy is impressive because it outperforms all other constant settings. The reason for the improvement is clear: at the beginning stage, the difference between two successive updates is significant because the model is far away from convergence. When the training comes to a stable point, the value of  $\lambda$  should be 1 such that the gradient eliminates the deviation towards the local minimizer.

#### 4.2 Estimating the global reference orientation

While applying SCAFFOLD [11] to train a model, we notice that the model update is biased to the fastest node under step-asynchronous settings. Given a model  $\mathbf{x}$ , some clients, e.g., client  $i$ , are close to a stable point such that the computed local reference orientation significantly deviates from the expected one, i.e.,  $\nabla F_i(\mathbf{x})$ . Regarding that the clients (client  $i$ ) with fewer local updates can better estimate the local orientation  $\nabla F_i(\mathbf{x})$ , the model prefers those with more local updates, which undermines the convergence property.

At the beginning of round  $t \in \{1, \dots, T\}$ , the centralized server broadcasts the model  $\tilde{\mathbf{x}}_t$  to all clients. To obtain an

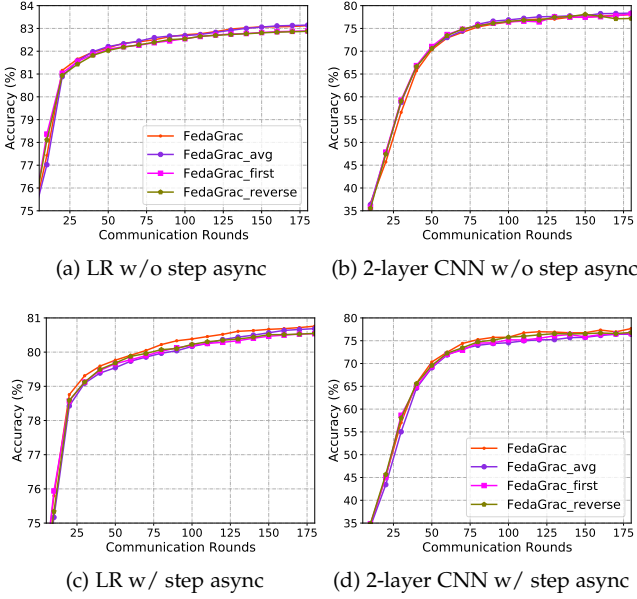


Fig. 3: Empirical evaluation for how to estimate the global reference orientation using Fashion-MNIST with convex (i.e., LR) and non-convex objectives (i.e., 2-layer CNN). The horizontal axis indicates the communication rounds, and the vertical axis shows the test accuracy in percentage. (a)(b) indicate the results when the clients run for the constant number of updates, and (c)(d) is when they perform various numbers of SGD steps. (Zoom in for the best view)

exact result of  $\nabla F(\tilde{\mathbf{x}}_t)$ , each client  $i \in \{1, \dots, M\}$  should provide an accurate estimation for  $\nabla F_i(\tilde{\mathbf{x}}_t)$ , or the bias of the estimation  $\nu^{(i)}$  can be eliminated by the sum, i.e.,  $\sum_{i=1}^M \omega_i \nu^{(i)}$ . Therefore, there are two practical ways to estimate  $\nabla F_i(\tilde{\mathbf{x}}_t)$  for client  $i$ , namely, (i) the first stochastic gradient, i.e.,  $\nabla f_i(\tilde{\mathbf{x}}_t, \varepsilon)$ , and (ii) the averaged stochastic gradient, i.e.,  $\frac{1}{K_i} \sum_{k=0}^{K_i-1} \nabla f_i(\mathbf{x}_{t,k}^{(i)}, \varepsilon_k^{(i)})$  in Line 11 of Algorithm 1. Based on these two strategies, we design and empirically evaluate four different schemes to find a proper estimation for the global reference orientation: (Note: faster or slower nodes are classified by whether the number of local updates is greater than the average updates)

- **FedagrAc** requires faster nodes to transmit the first stochastic gradient while the rest push the average one;
- **FedagrAc\_avg** (a.k.a. SCAFFOLD) requires all nodes to transmit the average stochastic gradient;
- **FedagrAc\_first** requires all nodes to transmit the first stochastic gradient;
- **FedagrAc\_reverse** requires faster nodes to transmit the average stochastic gradient while the rest push the first one.

Figure 3 presents the results of different strategies. As we can see, without step asynchronism, these four schemes do not have considerable differences. However, with step asynchronism, FedagrAc outperforms another three potential approaches under both convex and non-convex objectives. This is why Line 14 of Algorithm 1 is introduced.

To further reduce the communication overhead, the algorithm solely requests the faster nodes to upload the first stochastic gradient, while the rest can be computed via  $\frac{1}{\eta K_i} (\tilde{\mathbf{x}}_t - \mathbf{x}_{t,K_i}^{(i)}) - \lambda (\nu - \nu^{(i)})$  if  $\nu^{(i)}$  is preserved on the server.

## 5 THEORETICAL CONVERGENCE ANALYSIS

In this section, we analyze the convergence property of FedagrAc under both non-convex objectives and strongly-convex objectives for solving Problem (1). The details of the mathematical proof are provided in the supplementary materials with step-by-step explanations.

### 5.1 Mathematical expression for Algorithm 1

In Section 4, we describe the details in Algorithm 1. Below represents how to derive the recursive function step by step.

**Local reference orientation.** To ensure every local update can calibrate to the expected one, we should use the averaged local update such that after multiple local updates, the acquired model does not deviate from the expected orientation. Therefore, the local reference orientation is defined as:

$$\nu^{(i)} = \begin{cases} \frac{1}{K_i} \sum_{k=0}^{K_i-1} g_{t-1;k}^{(i)}, & K_i \leq \bar{K} \\ g_{t-1;0}^{(i)}, & \text{Otherwise} \end{cases} \quad (4)$$

**Global reference orientation.** SCAFFOLD [11] presents a remarkable performance with the aggregation of  $\nu^{(i)}$  for all  $i \in \{1, \dots, M\}$ . However, the approach presumably does not work due to step asynchronism, where local reference orientations deviated from the expected direction are dramatically various among clients. To avoid this issue, we let the faster node with more number of local updates transfer the initial gradient while others send the local reference orientation to the server, which can be formally written as:

$$\nu = \sum_{i, K_i \leq \bar{K}} \frac{\omega_i}{K_i} \sum_{k=0}^{K_i-1} g_{t-1;k}^{(i)} + \sum_{i, K_i > \bar{K}} \omega_i g_{t-1;0}^{(i)}$$

**Recursion function.** According to Line 9 in Algorithm 1, for client  $i$ , the recursion between two successive local updates can be presented as:

$$\mathbf{x}_{t,k+1}^{(i)} = \mathbf{x}_{t,k}^{(i)} - \eta \left[ g_{t;k}^{(i)} + \lambda (\nu - \nu^{(i)}) \right] \quad (5)$$

Then, based on the equation above, i.e., Equation (5), for client  $i$  with the local updates of  $K_i$ ,  $\mathbf{x}_{t,K_i}^{(i)} - \tilde{\mathbf{x}}_t$  can be formulated in mathematical expression as:

$$\begin{aligned} \mathbf{x}_{t,K_i}^{(i)} - \tilde{\mathbf{x}}_t &= \sum_{k=0}^{K_i-1} (\mathbf{x}_{t,k+1}^{(i)} - \mathbf{x}_{t,k}^{(i)}) \\ &= -\eta \sum_{k=0}^{K_i-1} g_{t;k}^{(i)} - \eta \lambda K_i (\nu - \nu^{(i)}) \end{aligned}$$

Finally, according to the definition in Problem (1), the recursion function between two successive global updates is the weighted average of all clients' models, which is written as:

$$\begin{aligned} \tilde{\mathbf{x}}_{t+1} - \tilde{\mathbf{x}}_t &= \sum_{i=1}^M \omega_i \mathbf{x}_{t,K_i}^{(i)} - \tilde{\mathbf{x}}_t \\ &= -\eta \sum_{i=1}^M \sum_{k=0}^{K_i-1} \omega_i g_{t;k}^{(i)} - \eta \lambda \bar{K} \nu + \eta \lambda \sum_{i=1}^M \omega_i K_i \nu^{(i)} \end{aligned}$$

## 5.2 Non-convex objectives

**Theorem 2** (Non-convex objectives). *Considering the same  $\mathbf{x}_1$  and  $\mathbf{x}_*$  as Theorem 1, under Assumption 1, 3 and 4, by setting  $\eta = \mathcal{O}\left(\sqrt{\frac{M}{TK}}\right)$ , the convergence rate of Algorithm 1 with step asynchronism for non-convex objectives is*

$$\begin{aligned} & \frac{1}{T} \sum_{t=1}^T \mathbb{E} \|\nabla F(\tilde{\mathbf{x}}_t)\|_2^2 \\ & \leq \mathcal{O}\left(\frac{F(\mathbf{x}_1) - F(\mathbf{x}_*)}{\lambda\sqrt{KMT}}\right) + \mathcal{O}\left(\frac{\sigma^2 L\sqrt{M}}{\lambda\sqrt{K^3T}} \sum_{i=1}^M \omega_i^2 K_i\right) \\ & \quad + \mathcal{O}\left(\frac{\sigma^2 L\lambda\sqrt{M}}{\sqrt{KT}} \sum_{i=1}^M \omega_i^2 \left(\frac{(\bar{K} - K_i)^2}{\bar{K}K_i} + 1\right)\right) \\ & \quad + \mathcal{O}\left(\frac{L^2\sigma^2 M}{\lambda\bar{K}^2 T} \sum_{i=1}^M \omega_i K_i^4\right) \\ & \quad + \mathcal{O}\left(\frac{L^2\sigma^2\lambda M}{\bar{K}^2 T} \sum_{i=1}^M \omega_i K_i^3 \left(K_i \sum_{j=1}^M \frac{\omega_j^2}{K_j} + 1\right)\right). \end{aligned} \quad (6)$$

*Proof.* See Appendix B for details.  $\square$

**Corollary 2.1.** *By setting  $\omega_1 = \dots = \omega_M = 1/M$  and  $\lambda = \mathcal{O}(1)$ , the following inequality holds under Theorem 2:*

$$\min_{t \in \{1, \dots, T\}} \mathbb{E} \|\nabla F(\tilde{\mathbf{x}}_t)\|_2^2 \leq \mathcal{O}\left(\frac{1}{\sqrt{MT\bar{K}}}\right). \quad (7)$$

**Remark** [10] states that FedaNova can achieve the convergence rate same as Equation 7, but there exists an explicit condition that  $\sum_{i=1}^M (\bar{K}/MK_i)$  is a constant when  $\omega_1 = \dots = \omega_M = 1/M$ . Let us consider an extreme case that the slow nodes locally update once, i.e.,  $K_i = 1$  for all  $i \in \{1, \dots, M-1\}$  while Client  $M$  can run for a very large number of times. This case is possible, for instance, a system consists of multiple Raspberry Pi and a single Nvidia GTX 3080Ti GPU, the computational difference between which can be up to a thousandfold. Under such situation, the aforementioned term should be bounded by  $\mathcal{O}(\bar{K})$  instead of  $\mathcal{O}(1)$  and therefore, the convergence rate for FedNova should be  $\mathcal{O}(\sqrt{\bar{K}/MT})$ . In comparison with Equation 7, Fedagrac achieves an increment up to  $\mathcal{O}(\bar{K})$ .

Furthermore, the algorithms such as FedAvg [24] and SCAFFOLD [11] that use the homogeneous setting achieve a convergence rate of  $\mathcal{O}(1/\sqrt{MTK_{\min}})$ . Obviously, Fedagrac admits better convergence rate as  $K_{\min} \leq \bar{K}$  always holds under heterogeneous computational resources. This is because our algorithm can fully utilize the computational resources from all participants such that it outperforms those algorithms that solely supports the homogeneous environment.

## 5.3 Strongly-convex objectives

**Theorem 3** (Strongly-convex objectives). *Considering the same  $\mathbf{x}_1$  and  $\mathbf{x}_*$  as Theorem 1, under Assumption 1, 2 and 3, by setting  $\lambda = 1$ ,  $\eta = \mathcal{O}(1/\mu LTK) \leq 1/L\bar{K}$ , the convergence rate of Algorithm 1 with step asynchronism for strongly-convex objectives is*

$$\begin{aligned} & \mathbb{E}[F(\tilde{\mathbf{x}}_T)] - F(\mathbf{x}_*) \\ & \leq \tilde{\mathcal{O}}\left(\mu \|\mathbf{x}_1 - \mathbf{x}_*\|_2^2 \exp\left(-\frac{\mu T}{L}\right) + \frac{\mathcal{H}}{\mu T} + \frac{\mathcal{P}}{\mu^2 T^2}\right), \end{aligned} \quad (8)$$

TABLE 3: Details for 2-layer CNN on Fashion-MNIST. Typically, Fashion-MNIST consists of grey-scale images possessing a single channel.

Layer	Output Shape	Trainable Parameters	Activation	Hyperparameters
Input	(1,28,28)	0		
Conv2d	(10, 24, 24)	260	ReLU	kernel size=5
MaxPool2d	(10, 12, 12)	0		kernel size=2
Conv2d	(20, 8, 8)	5020	ReLU	kernel size=5
Dropout2d	(20, 8, 8)	0		p=0.5
MaxPool2d	(20, 4, 4)	0		kernel size=2
Flatten	320	0		
Dense	50	16050	ReLU	
Dropout	50	0		p=0.5
Dense	10	510	softmax	

where

$$\begin{aligned} \mathcal{H} &= \frac{\sigma^2}{\bar{K}^2} \sum_{i=1}^M \omega_i^2 \left( K_i + \bar{K} + \frac{(\bar{K} - K_i)^2}{K_i} \right), \\ \mathcal{P} &= \frac{L^2\sigma^2}{\mu} \left( \sum_{i=1}^M \omega_i K_i^3 \right) \sum_{j=1}^M \frac{\omega_j^2}{K_j}. \end{aligned}$$

*Proof.* See Appendix C for details.  $\square$

**Corollary 3.1.** *By setting  $\omega_1 = \dots = \omega_M = 1/M$ , the following inequality holds under Theorem 3:*

$$\mathbb{E}[F(\tilde{\mathbf{x}}_T)] - F(\mathbf{x}_*) \leq \tilde{\mathcal{O}}\left(\frac{\sigma^2}{\mu MT\bar{K}}\right). \quad (9)$$

**Remark** Compared to FedNova [10] that has convergence theory only for non-convex objectives, we have established the rigorous convergence theory for our method Fedagrac on strongly-convex objectives. Compared with Theorem 1, Fedagrac not only converges to the optimal parameters, but also obtains a better convergence rate as  $\tilde{\mathcal{O}}(1/\bar{K}) \leq \tilde{\mathcal{O}}(1/K_{\min})$ .

## 6 EMPIRICAL EVALUATION

In this section, we conduct extensive experiments to evaluate the performance of Fedagrac in the real cases that are widely accepted by the existing studies. To further obtain an intuitive understanding of the numerical results, Fedagrac competes against other up-to-date benchmarks that are comparable under various settings. The code is implemented with PyTorch and available at <https://github.com/HarliWu/FedaGrac>.

### 6.1 Setup

**Datasets.** We leverage Fashion-MNIST [9] to run the preliminary experiments in the previous sections. This dataset comprises 60000  $28 \times 28$  grey-scale training images and 10000 test images, which can be categorized into ten classes related to the clothes type. In this section, we utilize two more datasets: a9a<sup>2</sup> and CIFAR-10 [57]. As a binary classification task, a9a consists of 32561 training samples and 16281 test samples, and each sample possesses 123 features. CIFAR-10 is a 10-category image classification task, constituting 60000  $32 \times 32$  color images divided into the training and test set with the size of 50000 and 10000, respectively.

**Models.** For the assessment of convex objectives, we train a logistic regression (LR) model using a9a. In addition, we

2. <https://www.csie.ntu.edu.tw/~cjlin/libsvmtools/datasets/>

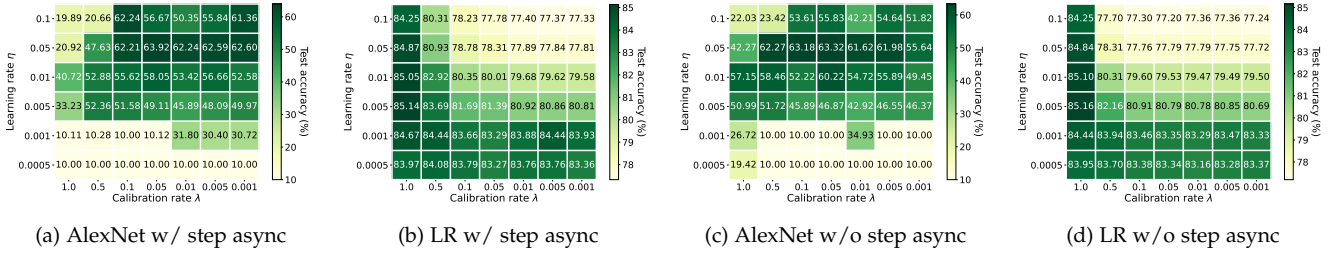


Fig. 4: Comparison of various setting combinations for learning rate  $\eta$  and calibration rate  $\lambda$  using DP1 data distribution under AlexNet and LR after 100 communication rounds. The horizontal index indicates the value of  $\lambda$  while the vertical index shows the value of  $\eta$ . The numeric in the box presents the averaged test accuracy of the last 10 rounds under the specific hyperparameter settings. The mean number of local updates is 500, and the variance with step asynchronism is 10000.

TABLE 4: Details for AlexNet on CIFAR-10. Output shape follows the format of (channel, height, width). Generally, color images like CIFAR-10 dataset are with three channels.

Layer	Output Shape	Trainable Parameters	Activation	Hyperparameters
Input	(3,32,32)	0		
Conv2d	(64, 8, 8)	23296	ReLU	kernel size=11, stride=4, padding=5
MaxPool2d	(64, 4, 4)	0		kernel size=2, stride=2
Conv2d	(192, 4, 4)	307392	ReLU	kernel size=5, padding=2
MaxPool2d	(192, 2, 2)	0		kernel size=2, stride=2
Conv2d	(384, 2, 2)	663936	ReLU	kernel size=3, padding=1
Conv2d	(256, 2, 2)	884992	ReLU	kernel size=3, padding=1
Conv2d	(256, 2, 2)	590080	ReLU	kernel size=3, padding=1
MaxPool2d	(256, 1, 1)	0		kernel size=2, stride=2
Flatten	256	0		
Dropout	256	0		$p = 0.5$
Dense	2048	526336	ReLU	
Dropout	2048	0		$p = 0.5$
Dense	2048	4196352	ReLU	
Dense	10	20490	softmax	

TABLE 5: Network architecture for VGG-19 on CIFAR-10.

Layer	Output Shape	Trainable Parameters	Activation	Hyperparameters
Input	(3,32,32)	0		
2 × Conv2d	(64, 32, 32)	38720	ReLU	kernel size=3; padding=1
MaxPool2d	(64, 16, 16)	0		kernel size=2, stride=2
2 × Conv2d	(128, 16, 16)	221440	ReLU	kernel size=3; padding=1
MaxPool2d	(128, 8, 8)	0		kernel size=2, stride=2
4 × Conv2d	(256, 8, 8)	2065408	ReLU	kernel size=3; padding=1
MaxPool2d	(256, 4, 4)	0		kernel size=2, stride=2
4 × Conv2d	(512, 4, 4)	8259584	ReLU	kernel size=3; padding=1
MaxPool2d	(512, 2, 2)	0		kernel size=2, stride=2
4 × Conv2d	(512, 2, 2)	9439232	ReLU	kernel size=3; padding=1
MaxPool2d	(512, 1, 1)	0		kernel size=2, stride=2
Flatten	512	0		
Dropout	512	0		$p = 0.5$
Dense	512	262656	ReLU	
Dropout	512	0		$p = 0.5$
Dense	512	262656	ReLU	
Dense	10	5130	softmax	

investigate the performance under non-convex objectives through an image classification task CIFAR-10 [57] with AlexNet [58] and VGG-19 [59], deep neural networks with total parameters of 7.21M and 20.55M, respectively. As for Fashion-MNIST, 2-layer CNN and LR are utilized to evaluate the performance under non-convex and convex objectives, respectively. Based on the dataset used, the details for 2-layer CNN, AlexNet and VGG-19 are separately described in Table 3, Table 4 and Table 5.

**Data Heterogeneity.** As for the non-i.i.d. settings, we adopt two different partitioned ways. The first one that we split the dataset across the clients follows the Dirichlet distribution with parameter 0.3, denoted as DP1. This approach is suitable for both datasets. The other method disjoints the dataset via sharding, and thus each client holds 5 classes. We let such a method be DP2 and ensure clients carry the same volume of data. It is worth noting that this partition is only compatible with CIFAR-10 because a9a is a binary classification challenge.

**Computational Heterogeneity.** To simulate a heterogeneous computing environment, we suppose the computation differences among workers follow the Gaussian distribution. Then, the number of local updates varies among clients and follows the normal distribution with predefined mean and variance. And the number of local updates may change over time for each client.

**Implementation and Hyperparameter Settings.** The experiments are conducted with an MPI-supported cluster with the configurations of 100GB RAM, 25 CPU cores, and 1 Nvidia P100 GPU. Based on the resource, we utilize 20 cores to act as clients and a single core as the federated server. Besides, the batch sizes throughout our experiments are set as 25 and 20 for CIFAR-10 and a9a, respectively. We choose FedAvg [6], FedNova [10], SCAFFOLD [11] and FedProx [51] as benchmarks and present the effectiveness of our proposed approach FedGrac. For a fair comparison, we compare these algorithms with the results when they achieve the best performance under the constant learning rates  $\{0.01, 0.008, 0.005\}$  and  $\{0.005, 0.001, 0.0005\}$  for AlexNet/VGG-19 and LR, respectively. And other required hyperparameters are also carefully picked from a set, such as the coefficient of the regularization term for FedProx in  $\{1, 0.1, 0.01\}$ . We specified other unmentioned but necessary settings in the captions of the figures and the tables.

## 6.2 Numerical Results

**Performance under Various combinations for learning rate and calibration rate.** As learning rate  $\eta$  and calibration rate  $\lambda$  need tuning in FedGrac, we first explore how to set both hyperparameters scientifically. Figure 4 depicts the test accuracy under various relations between  $\eta$  and  $\lambda$ . As we observe, the differences regarding the convexity are quite significant, e.g., AlexNet in Figure 4a and LR in Figure 4b, while the computation heterogeneity has minor influence on the selection of hyperparameters under the same model, e.g., AlexNet in Figure 4a and Figure 4c. Based on the acquired results, we discuss how to set the hyperparameters for FedGrac under convex or non-convex objectives.

Both Figure 4a and Figure 4c illustrate the performance under AlexNet with and without computational heterogeneity. In both cases, most  $\lambda$ s achieve the highest accuracy at  $\eta = 0.05$ , while some have the best performance at  $\eta = 0.01$ . When the learning rate initializes with a value



TABLE 6: The number of communication rounds when first achieving the target test accuracy under AlexNet and VGG-19. The computational capabilities among workers follow the Gaussian distribution with a mean of 500 and different variances (i.e.,  $V = 0$ ,  $V = 100$ , and  $V = 10000$ ) using two different data distributions (i.e., DP1 and DP2). Random mode indicates the number of local updates on a client varies among communication rounds, while fixed mode does not possess the feature. Each experiment runs for a maximum of 200 rounds.

Model	Data Distribution	Target Accuracy	Variance	Mode	Number of communication rounds ( $\downarrow$ )									
					FedaGrac	FedAvg	FedNova	SCAFFOLD	FedProx					
AlexNet	DP1	68%	V = 0	-		113		123		127		113		145
				V = 100	fixed		106		130		147		114	
			random			116		140		154		133		140
			V = 10000	fixed		126		156		172		141		142
				random		121		177		170		136		152
			AlexNet	DP2	70%	V = 0	-		152		183		186	
V = 100	fixed						111		179		119		124	
	random					112		200+		195		137		141
V = 10000	fixed					111		200+		113		131		145
	random					118		200+		200+		123		152
VGG-19	DP2	80%				V = 0	-		73		83		79	
			V = 100	fixed			73		75		72		66	
				random		73		85		74		78		102
			V = 10000	fixed		77		73		70		72		77
				random		71		85		76		72		99

smaller or equal to 0.001, most AlexNets seem untrained after 100 rounds because they are less likely to escape a saddle point. Although some portfolios successfully get out of the minima, they still cannot outperform the aforementioned settings because they may (i) trap into a non-optimal stable point or (ii) need a longer period to reach the optimal solution. A constant  $\lambda$  that performs well in all learning rates does not exist. However, when we shrink the choice of learning rate between 0.01 and 0.05,  $\lambda = 0.05$  has a remarkable performance. In our experiments, the calibration rate is chosen from  $\{0.01, \dots, 0.05\}$  depending on the algorithm’s performance.

Figure 4b and Figure 4d present the results under the convex objectives. Regardless of the step asynchronism,  $\lambda = 1$  always has remarkable performance for any learning rate. And it is noticeable that FedaGrac can obtain the best performance when  $\lambda = 1$  and  $\eta = 0.005$ . As for a  $\lambda \neq 1$ , FedaGrac can achieve better performance as the learning rate becomes smaller. With such a phenomenon, we hypothesize that FedaGrac cannot exactly reach the identical minimizer when  $\lambda \neq 1$  and approaches the expected point as the learning rate reduces.

**Performance under various data distributions.** Table 6 validates our algorithm under different data heterogeneities, i.e., DP1 and DP2 under AlexNet. The target accuracy is determined by the best performance that these five algorithms can achieve when they run a constant number of updates. By comparing each algorithm under these two data distributions, DP2 is more challenging for FedAvg and FedNova because the algorithms generally require more communication rounds to achieve the target. Even worse, these two algorithms cannot achieve the goal within 200 rounds in some DP2 settings. As for the regularization-based approach (i.e., FedProx) and the variance reduction approaches (i.e., FedaGrac and SCAFFOLD), the task shifting does not cause a distinct influence<sup>3</sup> in terms of the re-

quired communication rounds. As we can see in both cases with computational differences, FedaGrac demonstrates the superiority over other benchmarks.

**Performance under various neural networks.** In addition to exploring various data distributions based on Table 6, we investigate the performance of FedaGrac under different neural networks. As we notice, the approach in VGG-19 does not outperform all benchmarks in some computation heterogeneity cases. Specifically, it requires several more rounds than the best algorithm. An explanation for this phenomenon is that obtaining an 80%-accuracy VGG-19 on CIFAR-10 is not a difficult task. In contrast to getting an AlexNet with a test accuracy of 70%, the algorithms can adopt a greater learning rate to improve training efficiency. Since there are some restricted terms in FedaGrac, it is reasonable that our proposed algorithm cannot outperform the benchmarks. Meanwhile, it is common that some benchmarks cannot outperform FedAvg [60]. However, it is worth noting that, as presented in Figure 5, the faster algorithm may not surpass the slower ones in terms of the final test accuracy.

**Performance under various computational capabilities.** While adopting Gaussian distribution to tune the computation heterogeneity, we should manually set both mean and variance. To explore whether these two hyperparameters influence the algorithms’ performances, we conduct extensive experiments, and the relevant results are presented in Table 6 and Figure 5. Table 6 evaluates the performance under the computational capabilities with a constant mean of 500 and different variances, while Figure 5 assesses the convergence tendency under a fixed variance of 10000 and diverse means.

Table 6 presents the results given different variances with/without time-varying local updates. Our analysis is mainly based on AlexNet because it gives noticeable differences when the variances or the modes switch. Admittedly, these algorithms are not sensitive to whether the number of local updates is time-varying. However, it is worth noting that FedNova is vulnerable to time-varying settings in DP2.

3. The difference between the numbers of the communication rounds is less than 15%.

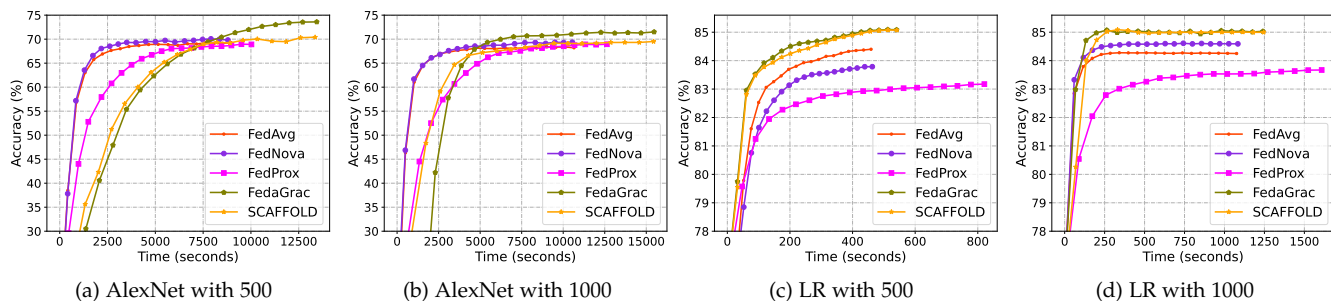


Fig. 5: Test accuracy v.s. Training time under different gaussian mean w.r.t. the fixed variance of 10000. Leftmost two figures: AlexNet using DP2; Rightmost two figures: LR using DP1. The number of local updates on a client is fixed and initialized at the beginning of the model training. Each algorithm runs for a total of 200 rounds, and the gap between two markers represents an interval of 10 communication rounds.

This is because a large learning rate may lead FedNova to a surrogate solution [50] such that FedNova has to adopt a smaller learning rate to achieve the target accuracy. In contrast to time-varying local updates, the variance plays an important role in training efficiency. When the variance becomes larger, it is likely that the algorithms require more communication rounds. Nevertheless, a greater variance sometimes improves the training efficiency of those algorithms which mitigate the client-drift effect, i.e., FedGrac, SCAFFOLD, and FedProx.

Figure 5 illustrates the entire training progress, i.e., the test accuracy with respect to the training time and the communication rounds under both convex and non-convex objectives. Our proposed algorithm achieves competitive accuracy compared to other baselines, despite a slow start likely taking place because the calibration is yet to settle the client-drift effects properly in the beginning. Although FedAvg and FedNova require half communication overhead as our proposed algorithm does, they cannot keep dominant alongside the training. Use AlexNet as an example (Figure 5a and 5b), and FedGrac is capable of achieving the same performance with fewer rounds. In addition, it is interesting to see FedProx consuming more time to implement 200 rounds than FedAvg. A reasonable explanation for this phenomenon is that extra computation is required by the regularization terms. As the model gets larger, this effect becomes minor since the communication consumption asymptotically occupies most training time (compare between LR (Figure 5c) and AlexNet (Figure 5a) for this heuristic conclusion). As a convex objective, LR depicts the issue of objective inconsistency (the latter two plots in Figure 5). The performances of FedAvg, FedNova, and FedProx are much worse than FedGrac and SCAFFOLD. With the increasing mean and the unchanged variance, the deterioration gets mitigation but cannot eliminate. As for the comparison between SCAFFOLD and our proposed method, the latter possesses dominance nearly all the time.

## 7 CONCLUSION

This paper introduces a new algorithm named FedGrac to tackle the challenges of both statistical heterogeneity and computation heterogeneity in FL. By calibrating the local client deviations according to an estimated global orientation in each communication round, the negative effect

of step asynchronism on model accuracy can be greatly mitigated, and the training process is remarkably accelerated. We establish the theoretical convergence rate of FedGrac. The results imply that FedGrac admits a faster convergence rate and has a better tolerance to computation heterogeneity than the state-of-the-art approaches. Extensive experiments are also conducted to validate the advantages of FedGrac.

## ACKNOWLEDGMENTS

The authors would like to thank Shiqi He for the useful discussion and the anonymous reviewers for their constructive comments. This research was supported by fundings from the Key-Area Research and Development Program of Guangdong Province (No. 2021B0101400003), Hong Kong RGC Research Impact Fund (No. R5060-19), Areas of Excellence Scheme (AoE/E-601/22-R), General Research Fund (No. 152203/20E, 152244/21E, 152169/22E), Shenzhen Science and Technology Innovation Commission (JCYJ20200109142008673), the National Natural Science Foundation of China (Grant 62102131), and Natural Science Foundation of Jiangsu Province (Grant BK20210361).

## REFERENCES

- [1] Y. Liu, A. Huang, Y. Luo, H. Huang, Y. Liu, Y. Chen, L. Feng, T. Chen, H. Yu, and Q. Yang, "Fedvision: An online visual object detection platform powered by federated learning," in *Proceedings of the AAAI Conference on Artificial Intelligence*, vol. 34, no. 08, 2020, pp. 13 172–13 179.
- [2] P. Yu and Y. Liu, "Federated object detection: Optimizing object detection model with federated learning," in *Proceedings of the 3rd International Conference on Vision, Image and Signal Processing*, 2019, pp. 1–6.
- [3] F. Liu, X. Wu, S. Ge, W. Fan, and Y. Zou, "Federated learning for vision-and-language grounding problems," in *Proceedings of the AAAI Conference on Artificial Intelligence*, vol. 34, no. 07, 2020, pp. 11 572–11 579.
- [4] X. Wu, Z. Liang, and J. Wang, "Fedmed: A federated learning framework for language modeling," *Sensors*, vol. 20, no. 14, p. 4048, 2020.
- [5] M. Chen, A. T. Suresh, R. Mathews, A. Wong, C. Allauzen, F. Beaufays, and M. Riley, "Federated learning of n-gram language models," *arXiv preprint arXiv:1910.03432*, 2019.
- [6] B. McMahan, E. Moore, D. Ramage, S. Hampson, and B. A. y Arcas, "Communication-efficient learning of deep networks from decentralized data," in *Artificial intelligence and statistics*. PMLR, 2017, pp. 1273–1282.

- [7] X. Li, K. Huang, W. Yang, S. Wang, and Z. Zhang, "On the convergence of fedavg on non-iid data," *arXiv preprint arXiv:1907.02189*, 2019.
- [8] Z. Chai, H. Fayyaz, Z. Fayyaz, A. Anwar, Y. Zhou, N. Baracaldo, H. Ludwig, and Y. Cheng, "Towards taming the resource and data heterogeneity in federated learning," in *2019 {USENIX} Conference on Operational Machine Learning (OpML 19)*, 2019, pp. 19–21.
- [9] H. Xiao, K. Rasul, and R. Vollgraf, "Fashion-mnist: a novel image dataset for benchmarking machine learning algorithms," 2017.
- [10] J. Wang, Q. Liu, H. Liang, G. Joshi, and H. V. Poor, "Tackling the objective inconsistency problem in heterogeneous federated optimization," *Advances in Neural Information Processing Systems*, vol. 33, 2020.
- [11] S. P. Karimireddy, S. Kale, M. Mohri, S. Reddi, S. Stich, and A. T. Suresh, "Scaffold: Stochastic controlled averaging for federated learning," in *International Conference on Machine Learning*. PMLR, 2020, pp. 5132–5143.
- [12] S. Guo and Z. Qu, *Edge Learning for Distributed Big Data Analytics: Theory, Algorithms, and System Design*. Cambridge University Press, 2022.
- [13] R. Han, S. Li, X. Wang, C. H. Liu, G. Xin, and L. Y. Chen, "Accelerating gossip-based deep learning in heterogeneous edge computing platforms," *IEEE Transactions on Parallel and Distributed Systems*, vol. 32, no. 7, pp. 1591–1602, 2020.
- [14] W. Y. B. Lim, J. S. Ng, Z. Xiong, J. Jin, Y. Zhang, D. Niyato, C. Leung, and C. Miao, "Decentralized edge intelligence: A dynamic resource allocation framework for hierarchical federated learning," *IEEE Transactions on Parallel and Distributed Systems*, vol. 33, no. 3, pp. 536–550, 2021.
- [15] H. Wang, Z. Qu, Q. Zhou, H. Zhang, B. Luo, W. Xu, S. Guo, and R. Li, "A comprehensive survey on training acceleration for large machine learning models in iots," *IEEE Internet of Things Journal*, 2021.
- [16] H. Wang, Z. Qu, S. Guo, N. Wang, R. Li, and W. Zhuang, "Losp: Overlap synchronization parallel with local compensation for fast distributed training," *IEEE Journal on Selected Areas in Communications*, vol. 39, no. 8, pp. 2541–2557, 2021.
- [17] Z. Qu, S. Guo, H. Wang, B. Ye, Y. Wang, A. Zomaya, and B. Tang, "Partial synchronization to accelerate federated learning over relay-assisted edge networks," *IEEE Transactions on Mobile Computing*, pp. 1–1, 2021.
- [18] J. Zhang, S. Guo, Z. Qu, D. Zeng, H. Wang, Q. Liu, and A. Y. Zomaya, "Adaptive vertical federated learning on unbalanced features," *IEEE Transactions on Parallel and Distributed Systems*, vol. 33, no. 12, pp. 4006–4018, 2022.
- [19] J. Zhang, S. Guo, X. Ma, H. Wang, W. Xu, and F. Wu, "Parameterized knowledge transfer for personalized federated learning," *Advances in Neural Information Processing Systems*, vol. 34, 2021.
- [20] C. T. Dinh, N. Tran, and J. Nguyen, "Personalized federated learning with moreau envelopes," *Advances in Neural Information Processing Systems*, vol. 33, pp. 21 394–21 405, 2020.
- [21] X. Tang, S. Guo, and J. Guo, "Personalized federated learning with contextualized generalization," *arXiv preprint arXiv:2106.13044*, 2021.
- [22] J. Konečný, B. McMahan, and D. Ramage, "Federated optimization: Distributed optimization beyond the datacenter," *arXiv preprint arXiv:1511.03575*, 2015.
- [23] S. U. Stich, "Local sgd converges fast and communicates little," in *International Conference on Learning Representations*, 2018.
- [24] H. Yu, S. Yang, and S. Zhu, "Parallel restarted sgd with faster convergence and less communication: Demystifying why model averaging works for deep learning," in *Proceedings of the AAAI Conference on Artificial Intelligence*, vol. 33, no. 01, 2019, pp. 5693–5700.
- [25] F. Zhou and G. Cong, "On the convergence properties of a k-step averaging stochastic gradient descent algorithm for nonconvex optimization," in *Proceedings of the 27th International Joint Conference on Artificial Intelligence*, 2018, pp. 3219–3227.
- [26] A. Khaled, K. Mishchenko, and P. Richtárik, "Tighter theory for local sgd on identical and heterogeneous data," in *International Conference on Artificial Intelligence and Statistics*. PMLR, 2020, pp. 4519–4529.
- [27] X. Gu, K. Huang, J. Zhang, and L. Huang, "Fast federated learning in the presence of arbitrary device unavailability," *arXiv preprint arXiv:2106.04159*, 2021.
- [28] D. Alistarh, D. Grubic, J. Li, R. Tomioka, and M. Vojnovic, "Qsgd: Communication-efficient sgd via gradient quantization and encoding," *Advances in Neural Information Processing Systems*, vol. 30, 2017.
- [29] D. Basu, D. Data, C. Karakus, and S. Diggavi, "Qsparse-local-sgd: Distributed sgd with quantization, sparsification and local computations," *Advances in Neural Information Processing Systems*, vol. 32, 2019.
- [30] F. Wu, S. He, S. Guo, Z. Qu, H. Wang, W. Zhuang, and J. Zhang, "Sign bit is enough: a learning synchronization framework for multi-hop all-reduce with ultimate compression," in *Proceedings of the 59th ACM/IEEE Design Automation Conference*, 2022, pp. 193–198.
- [31] S. U. Stich, J.-B. Cordonnier, and M. Jaggi, "Sparsified sgd with memory," *Advances in Neural Information Processing Systems*, vol. 31, 2018.
- [32] J. Wangni, J. Wang, J. Liu, and T. Zhang, "Gradient sparsification for communication-efficient distributed optimization," *Advances in Neural Information Processing Systems*, vol. 31, 2018.
- [33] Y. Zhou, Q. Ye, and J. C. Lv, "Communication-efficient federated learning with compensated overlap-fedavg," *IEEE Transactions on Parallel and Distributed Systems*, 2021.
- [34] X. Wu, X. Yao, and C.-L. Wang, "Fedscr: Structure-based communication reduction for federated learning," *IEEE Transactions on Parallel and Distributed Systems*, vol. 32, no. 7, pp. 1565–1577, 2020.
- [35] H. Wang, S. Guo, Z. Qu, R. Li, and Z. Liu, "Error-compensated sparsification for communication-efficient decentralized training in edge environment," *IEEE Transactions on Parallel and Distributed Systems*, 2021.
- [36] F. Wu, S. He, Y. Yang, H. Wang, Z. Qu, S. Guo, and W. Zhuang, "On the convergence of quantized parallel restarted sgd for central server free distributed training," *arXiv preprint arXiv:2004.09125*, 2020.
- [37] Y. Zhao, M. Li, L. Lai, N. Suda, D. Civin, and V. Chandra, "Federated learning with non-iid data," *arXiv preprint arXiv:1806.00582*, 2018.
- [38] W. Liu, L. Chen, Y. Chen, and W. Zhang, "Accelerating federated learning via momentum gradient descent," *IEEE Transactions on Parallel and Distributed Systems*, vol. 31, no. 8, pp. 1754–1766, 2020.
- [39] E. Gorbunov, F. Hanzely, and P. Richtárik, "A unified theory of sgd: Variance reduction, sampling, quantization and coordinate descent," in *International Conference on Artificial Intelligence and Statistics*. PMLR, 2020, pp. 680–690.
- [40] D. Cheng, S. Li, H. Zhang, F. Xia, and Y. Zhang, "Why dataset properties bound the scalability of parallel machine learning training algorithms," *IEEE Transactions on Parallel and Distributed Systems*, vol. 32, no. 7, pp. 1702–1712, 2021.
- [41] X. Liang, S. Shen, J. Liu, Z. Pan, E. Chen, and Y. Cheng, "Variance reduced local sgd with lower communication complexity," *arXiv preprint arXiv:1912.12844*, 2019.
- [42] A. Ghosh, J. Chung, D. Yin, and K. Ramchandran, "An efficient framework for clustered federated learning," *Advances in Neural Information Processing Systems*, vol. 33, 2020.
- [43] T. Murata and T. Suzuki, "Bias-variance reduced local sgd for less heterogeneous federated learning," *arXiv preprint arXiv:2102.03198*, 2021.
- [44] Y. Fraboni, R. Vidal, L. Kameni, and M. Lorenzi, "Clustered sampling: Low-variance and improved representativity for clients selection in federated learning," *arXiv preprint arXiv:2105.05883*, 2021.
- [45] H. Wang, Z. Kaplan, D. Niu, and B. Li, "Optimizing federated learning on non-iid data with reinforcement learning," in *IEEE INFOCOM 2020-IEEE Conference on Computer Communications*. IEEE, 2020, pp. 1698–1707.
- [46] T. Huang, W. Lin, W. Wu, L. He, K. Li, and A. Y. Zomaya, "An efficiency-boosting client selection scheme for federated learning with fairness guarantee," *IEEE Transactions on Parallel and Distributed Systems*, vol. 32, no. 7, pp. 1552–1564, 2020.
- [47] Y. Deng, F. Lyu, J. Ren, H. Wu, Y. Zhou, Y. Zhang, and X. Shen, "Auction: Automated and quality-aware client selection framework for efficient federated learning," *IEEE Transactions on Parallel and Distributed Systems*, vol. 33, no. 8, pp. 1996–2009, 2021.
- [48] Q. Zhou, S. Guo, Z. Qu, P. Li, L. Li, M. Guo, and K. Wang, "Petrel: Heterogeneity-aware distributed deep learning via hybrid synchronization," *IEEE Transactions on Parallel and Distributed Systems*, vol. 32, no. 5, pp. 1030–1043, 2020.
- [49] W. Wu, L. He, W. Lin, and R. Mao, "Accelerating federated learning over reliability-agnostic clients in mobile edge computing

systems," *IEEE Transactions on Parallel and Distributed Systems*, vol. 32, no. 7, pp. 1539–1551, 2020.

- [50] A. Mitra, R. Jaafar, G. Pappas, and H. Hassani, "Linear convergence in federated learning: Tackling client heterogeneity and sparse gradients," *Advances in Neural Information Processing Systems*, vol. 34, 2021.
- [51] T. Li, A. K. Sahu, M. Zaheer, M. Sanjabi, A. Talwalkar, and V. Smith, "Federated optimization in heterogeneous networks," *Proceedings of Machine Learning and Systems*, vol. 2, pp. 429–450, 2020.
- [52] E. Diao, J. Ding, and V. Tarokh, "Heterofi: Computation and communication efficient federated learning for heterogeneous clients," *arXiv preprint arXiv:2010.01264*, 2020.
- [53] S. J. Reddi, Z. Charles, M. Zaheer, Z. Garrett, K. Rush, J. Konečný, S. Kumar, and H. B. McMahan, "Adaptive federated optimization," in *International Conference on Learning Representations*, 2020.
- [54] H. Wang, S. Guo, and R. Li, "Osp: Overlapping computation and communication in parameter server for fast machine learning," in *Proceedings of the 48th International Conference on Parallel Processing*, 2019, pp. 1–10.
- [55] M. Zinkevich, M. Weimer, L. Li, and A. Smola, "Parallelized stochastic gradient descent," *Advances in neural information processing systems*, vol. 23, 2010.
- [56] L. Bottou, "Large-scale machine learning with stochastic gradient descent," in *Proceedings of COMPSTAT 2010*. Springer, 2010, pp. 177–186.
- [57] A. Krizhevsky, G. Hinton *et al.*, "Learning multiple layers of features from tiny images," 2009.
- [58] A. Krizhevsky, I. Sutskever, and G. E. Hinton, "Imagenet classification with deep convolutional neural networks," *Advances in neural information processing systems*, vol. 25, 2012.
- [59] K. Simonyan and A. Zisserman, "Very deep convolutional networks for large-scale image recognition," *arXiv preprint arXiv:1409.1556*, 2014.
- [60] Q. Li, Y. Diao, Q. Chen, and B. He, "Federated learning on non-iid data silos: An experimental study," *arXiv preprint arXiv:2102.02079*, 2021.

## APPENDIX A PROOF OF THEOREM 1

The following lemma describes the relationship among three different parameters under strongly-convex function:

**Lemma 1.** *Under Assumption 1 and Assumption 2, given  $\mathbf{a}, \mathbf{b}, \mathbf{c} \in \mathbb{R}^d$ , the following formula holds under the strongly-convex objectives  $F$ :*

$$\langle \nabla F(\mathbf{a}), \mathbf{b} - \mathbf{c} \rangle \leq F(\mathbf{b}) - F(\mathbf{c}) - \frac{\mu}{4} \|\mathbf{b} - \mathbf{c}\|_2^2 + L \|\mathbf{a} - \mathbf{c}\|_2^2 \quad (10)$$

*Proof.* With  $\mathbf{a}, \mathbf{b}$  and  $\mathbf{c}$  that are within the domain of  $F$ , we can get the following inequalities that come from Assumption 1 and Assumption 2, respectively:

$$\begin{aligned} \langle \nabla F(\mathbf{a}), \mathbf{b} - \mathbf{a} \rangle &\leq F(\mathbf{b}) - F(\mathbf{a}) + \frac{L}{2} \|\mathbf{a} - \mathbf{b}\|_2^2 \\ \langle \nabla F(\mathbf{a}), \mathbf{a} - \mathbf{c} \rangle &\leq F(\mathbf{a}) - F(\mathbf{c}) - \frac{\mu}{2} \|\mathbf{a} - \mathbf{c}\|_2^2 \end{aligned}$$

By a formula that

$$\|\mathbf{a} - \mathbf{b}\|_2^2 \leq 2\|\mathbf{a} - \mathbf{c}\|_2^2 + 2\|\mathbf{b} - \mathbf{c}\|_2^2$$

we have:

$$\langle \nabla F(\mathbf{a}), \mathbf{b} - \mathbf{c} \rangle \leq F(\mathbf{b}) - F(\mathbf{c}) - \frac{\mu}{4} \|\mathbf{b} - \mathbf{c}\|_2^2 + \frac{L + \mu}{2} \|\mathbf{a} - \mathbf{c}\|_2^2$$

The inequality holds when  $L \geq \mu$ .  $\square$

The update rule for FedAvg under heterogeneous steps:

$$\mathbf{x}_{t+1} = \mathbf{x}_t - \eta \sum_{i=1}^M \omega_i \sum_{k=0}^{K_i-1} \nabla f_i(\mathbf{x}_{t,k}^{(i)}, \varepsilon_k^{(i)}) \quad (11)$$

Therefore, the bound established for  $\mathbb{E} \|\mathbf{x}_{t+1} - \mathbf{x}_*\|_2^2$  should be:

$$\begin{aligned} &\mathbb{E} \|\mathbf{x}_{t+1} - \mathbf{x}_*\|_2^2 \\ &= \mathbb{E} \left\| \mathbf{x}_t - \eta \sum_{i=1}^M \omega_i \sum_{k=0}^{K_i-1} \nabla f_i(\mathbf{x}_{t,k}^{(i)}, \varepsilon_k^{(i)}) - \mathbf{x}_* \right\|_2^2 \\ &= \mathbb{E} \|\mathbf{x}_t - \mathbf{x}_*\|_2^2 + \mathbb{E} \left\| \eta \sum_{i=1}^M \omega_i \sum_{k=0}^{K_i-1} \nabla f_i(\mathbf{x}_{t,k}^{(i)}, \varepsilon_k^{(i)}) \right\|_2^2 \\ &\quad - 2\mathbb{E} \left\langle \mathbf{x}_t - \mathbf{x}_*, \eta \sum_{i=1}^M \omega_i \sum_{k=0}^{K_i-1} \nabla f_i(\mathbf{x}_{t,k}^{(i)}, \varepsilon_k^{(i)}) \right\rangle \\ &= \mathbb{E} \|\mathbf{x}_t - \mathbf{x}_*\|_2^2 + \eta^2 \sum_{i=1}^M \omega_i^2 K_i \sigma^2 \end{aligned} \quad (12)$$

$$+ \eta^2 \mathbb{E} \left\| \sum_{i=1}^M \sum_{k=0}^{K_i-1} \omega_i \nabla F_i(\mathbf{x}_{t,k}^{(i)}) \right\|_2^2 \quad (13)$$

$$- 2\mathbb{E} \left\langle \mathbf{x}_t - \mathbf{x}_*, \eta \sum_{i=1}^M \omega_i \sum_{k=0}^{K_i-1} \nabla F_i(\mathbf{x}_{t,k}^{(i)}) \right\rangle \quad (14)$$

We first find an upper bound for  $\mathcal{A}_1$  in accordance with Lemma 1:

$$\begin{aligned} \mathcal{A}_1 &= 2\eta \sum_{i=1}^M \sum_{k=0}^{K_i-1} \omega_i \cdot \mathbb{E} \langle \mathbf{x}_* - \mathbf{x}_t, \nabla F_i(\mathbf{x}_{t,k}^{(i)}) \rangle \\ &\leq 2\eta \sum_{i=1}^M \omega_i K_i [F_i(\mathbf{x}_*) - F_i(\mathbf{x}_t)] - \frac{\eta \mu \bar{K}}{2} \|\mathbf{x}_t - \mathbf{x}_*\|_2^2 \end{aligned} \quad (15)$$

$$+ 2\eta L \underbrace{\sum_{i=1}^M \sum_{k=0}^{K_i-1} \omega_i \mathbb{E} \|\mathbf{x}_{t,k}^{(i)} - \mathbf{x}_t\|_2^2}_{\mathcal{A}_3} \quad (16)$$

To find the maximum value for  $\mathcal{A}_3$ , we bound  $\mathbb{E} \|\mathbf{x}_{t,k}^{(i)} - \mathbf{x}_t\|_2^2$  for  $k \in \{1, \dots, K_i\}$  via the following inequality:

$$\begin{aligned} &\mathbb{E} \|\mathbf{x}_{t,k}^{(i)} - \mathbf{x}_t\|_2^2 \\ &= \mathbb{E} \left\| \mathbf{x}_{t,k-1}^{(i)} - \eta \nabla f_i(\mathbf{x}_{t,k-1}^{(i)}, \varepsilon_{k-1}^{(i)}) - \mathbf{x}_t \right\|_2^2 \\ &\leq \mathbb{E} \left\| \mathbf{x}_{t,k-1}^{(i)} - \mathbf{x}_t - \eta \nabla F_i(\mathbf{x}_{t,k-1}^{(i)}) \right\|_2^2 + \eta^2 \sigma^2 \\ &\stackrel{(a)}{\leq} \left( 1 + \frac{1}{K_i - 1} \right) \|\mathbf{x}_{t,k-1}^{(i)} - \mathbf{x}_t\|_2^2 + \eta^2 \sigma^2 \\ &\quad + K_i \eta^2 \left( 2 \|\nabla F_i(\mathbf{x}_{t,k-1}^{(i)}) - \nabla F_i(\tilde{\mathbf{x}}_t)\|_2^2 + 2 \|\nabla F_i(\tilde{\mathbf{x}}_t)\|_2^2 \right) \\ &\leq \left( 1 + \frac{1}{K_i - 1} + 2K_i \eta^2 L^2 \right) \|\mathbf{x}_{t,k-1}^{(i)} - \mathbf{x}_t\|_2^2 \\ &\quad + \eta^2 \sigma^2 + 2K_i \eta^2 \|\nabla F_i(\mathbf{x}_t)\|_2^2 \end{aligned}$$

where (a) follows triangle inequality, i.e.,  $(x + y)^2 \leq (1 + k)x^2 + (1 + 1/k)y^2$  for all  $k > 0$ . By setting  $\eta \leq \sqrt{\frac{1}{2K_{\max}(K_{\max}-1)L^2}}$ , we have:

$$\mathbb{E} \|\mathbf{x}_{t,k}^{(i)} - \mathbf{x}_t\|_2^2$$

$$\begin{aligned}
&\leq \sum_{\kappa=0}^{k-1} \left(1 + \frac{2}{K_i - 1}\right)^\kappa \left(\eta^2 \sigma^2 + 2K_i \eta^2 \|\nabla F_i(\mathbf{x}_t)\|_2^2\right) \\
&= \frac{\left(1 + \frac{2}{K_i - 1}\right)^k - 1}{\frac{2}{K_i - 1}} \left(\eta^2 \sigma^2 + 2K_i \eta^2 \|\nabla F_i(\mathbf{x}_t)\|_2^2\right) \\
&\stackrel{(a)}{\leq} 4K_i \left(\eta^2 \sigma^2 + 2K_i \eta^2 \|\nabla F_i(\mathbf{x}_t)\|_2^2\right) \quad (17)
\end{aligned}$$

where (a) is on account for:

$$\left(1 + \frac{2}{K_i - 1}\right)^{K_i} \leq 9 \quad \text{for} \quad K_i \geq 2$$

Based on the derivative above, we can obtain the bound for  $\mathcal{A}_3$  with:

$$\begin{aligned}
\mathcal{A}_3 &\leq \sum_{i=1}^M \sum_{k=0}^{K_i-1} \omega_i \cdot 4K_i \left(\eta^2 \sigma^2 + 2K_i \eta^2 \|\nabla F_i(\mathbf{x}_t)\|_2^2\right) \\
&= 4\eta^2 \sigma^2 \sum_{i=1}^M \omega_i K_i^2 + 8\eta^2 \sum_{i=1}^M \omega_i K_i^3 \|\nabla F_i(\mathbf{x}_t)\|_2^2
\end{aligned}$$

Therefore, the bound for  $\mathcal{A}_1$  can be further simplified as:

$$\begin{aligned}
\mathcal{A}_1 &\leq 2\eta \sum_{i=1}^M \omega_i K_i [F_i(\mathbf{x}^*) - F_i(\mathbf{x}_t)] - \frac{\eta\mu\bar{K}}{2} \|\mathbf{x}_t - \mathbf{x}_*\|_2^2 \\
&\quad + 2\eta L \left[ 4\eta^2 \sigma^2 \sum_{i=1}^M \omega_i K_i^2 + 8\eta^2 \sum_{i=1}^M \omega_i K_i^3 \|\nabla F_i(\mathbf{x}_t)\|_2^2 \right]
\end{aligned}$$

Next, we consider the bound for  $\mathcal{A}_2$ :

$$\begin{aligned}
\mathcal{A}_2 &\leq 2\eta^2 \cdot \mathbb{E} \left\| \sum_{i=1}^M \sum_{k=0}^{K_i-1} \omega_i \left[ \nabla F_i(\mathbf{x}_{t,k}^{(i)}) - \nabla F_i(\mathbf{x}_t) \right] \right\|_2^2 \\
&\quad + 2\eta^2 \cdot \mathbb{E} \left\| \sum_{i=1}^M \omega_i K_i \nabla F_i(\mathbf{x}_t) \right\|_2^2 \\
&\leq 2\eta^2 L^2 \sum_{i=1}^M \sum_{k=0}^{K_i-1} \omega_i K_i \cdot \mathbb{E} \left\| \mathbf{x}_{t,k}^{(i)} - \mathbf{x}_t \right\|_2^2 \\
&\quad + 2\eta^2 \sum_{i=1}^M \omega_i K_i^2 \|\nabla F_i(\tilde{\mathbf{x}}_t)\|_2^2 \\
&\leq 8\eta^4 L^2 \sigma^2 \sum_{i=1}^M \omega_i K_i^3 \\
&\quad + 2\eta^2 \sum_{i=1}^M \omega_i K_i^2 (1 + 8\eta^2 L^2 K_i^2) \|\nabla F_i(\tilde{\mathbf{x}}_t)\|_2^2
\end{aligned}$$

Therefore, plugging  $\mathcal{A}_1$  and  $\mathcal{A}_2$  into the inequality bound for  $\mathbb{E} \|\mathbf{x}_{t+1} - \mathbf{x}^*\|_2^2$ , the bound can be simplified as:

$$\begin{aligned}
&\mathbb{E} \|\mathbf{x}_{t+1} - \mathbf{x}^*\|_2^2 \\
&\leq \left(1 - \frac{\eta\mu\bar{K}}{2}\right) \mathbb{E} \|\mathbf{x}_t - \mathbf{x}^*\|_2^2 \\
&\quad + 2\eta \sum_{i=1}^M \omega_i K_i [F_i(\mathbf{x}^*) - F_i(\mathbf{x}_t)] \\
&\quad + 8\eta^3 \sigma^2 L \sum_{i=1}^M \omega_i K_i^2 + \eta^2 \sigma^2 \sum_{i=1}^M \omega_i^2 K_i \\
&\quad + 8\eta^4 L^2 \sigma^2 \sum_{i=1}^M \omega_i K_i^3 + 16\eta^3 L \sum_{i=1}^M \omega_i K_i^3 \|\nabla F_i(\mathbf{x}_t)\|_2^2
\end{aligned}$$

$$+ 2\eta^2 \sum_{i=1}^M \omega_i K_i^2 (1 + 8\eta^2 L^2 K_i) \|\nabla F_i(\mathbf{x}_t)\|_2^2$$

Divided  $\bar{K}$  on the both side, we can obtain the following formula:

$$\begin{aligned}
&\frac{1}{\bar{K}} \sum_{i=1}^M \omega_i K_i [F_i(\mathbf{x}^*) - F_i(\mathbf{x}_t)] \\
&\leq \frac{1}{\bar{K}\eta} \left(1 - \frac{\eta\mu\bar{K}}{2}\right) \mathbb{E} \|\mathbf{x}_t - \mathbf{x}^*\|_2^2 - \frac{1}{\bar{K}\eta} \mathbb{E} \|\mathbf{x}_{t+1} - \mathbf{x}^*\|_2^2 \\
&\quad + \frac{8\eta^2 \sigma^2 L}{\bar{K}} \sum_{i=1}^M \omega_i K_i^2 + \frac{\eta\sigma^2}{\bar{K}} \sum_{i=1}^M \omega_i^2 K_i \\
&\quad + \frac{8\eta^3 L^2 \sigma^2}{\bar{K}} \sum_{i=1}^M \omega_i K_i^3
\end{aligned}$$

By applying Lemma 1 from [11], we can obtain the desirable result. It is worthwhile to mention a formula below that supports the reason why the gap exists between a stable point and the optimal solution:

$$\begin{aligned}
&\sum_{i=1}^M \omega_i K_i (F_i(\mathbf{x}_t) - F_i(\mathbf{x}_*)) \\
&\geq K_{\min} \sum_{i=1}^M \omega_i (F_i(\mathbf{x}_t) - F_i(\mathbf{x}_*)) \\
&\quad - \sum_{i=1}^M \omega_i (K_i - K_{\min}) F_i(\mathbf{x}_*)
\end{aligned}$$

The inequality holds when the value of the objective function is non-negative. This formula indicates that the data heterogeneity can be eliminated under homogeneous computing environment since for all  $i \in \{1, \dots, M\}$ ,  $K_i = K_{\min}$ . Thus, in this case, we can obtain the same convergence order as [11].

## APPENDIX B PROOF OF THEOREM 2

According to  $L$ -smooth, we have:

$$\begin{aligned}
&\mathbb{E} [F(\tilde{\mathbf{x}}_{t+1})] - F(\tilde{\mathbf{x}}_t) \\
&\leq \mathbb{E} \langle \nabla F(\tilde{\mathbf{x}}_t), \tilde{\mathbf{x}}_{t+1} - \tilde{\mathbf{x}}_t \rangle + \frac{L}{2} \mathbb{E} \|\tilde{\mathbf{x}}_{t+1} - \tilde{\mathbf{x}}_t\|_2^2 \quad (18)
\end{aligned}$$

**The first term of Equation (18).** We firstly find the bound for the first term of Equation (18):

$$\begin{aligned}
&\mathbb{E} \langle \nabla F(\tilde{\mathbf{x}}_t), \tilde{\mathbf{x}}_{t+1} - \tilde{\mathbf{x}}_t \rangle \\
&= \mathbb{E} \left\langle \nabla F(\tilde{\mathbf{x}}_t), -\eta \sum_{i=1}^M \sum_{k=0}^{K_i-1} \omega_i \nabla F_i(\mathbf{x}_{t,k}^{(i)}) \right. \\
&\quad + \eta\lambda \sum_{i=1}^M \omega_i \sum_{\kappa=0}^{K_i-1} \nabla F_i(\mathbf{x}_{t-1,\kappa}^{(i)}) - \eta\lambda\bar{K} \nabla F(\tilde{\mathbf{x}}_{t-1}) \\
&\quad \left. - \eta\lambda\bar{K} \sum_{i,K_i \leq \bar{K}} \sum_{k=0}^{K_i-1} \frac{\omega_i}{K_i} \left( \nabla F_i(\mathbf{x}_{t-1,k}^{(i)}) - \nabla F_i(\tilde{\mathbf{x}}_{t-1}) \right) \right\rangle \\
&= -\frac{\eta\lambda}{\bar{K}} \mathbb{E} \left\langle \bar{K} \nabla F(\tilde{\mathbf{x}}_t), \sum_{i=1}^M \sum_{k=0}^{K_i-1} \omega_i \nabla F_i(\mathbf{x}_{t,k}^{(i)}) \right. \\
&\quad \left. - \sum_{i=1}^M \sum_{\kappa=0}^{K_i-1} \omega_i \nabla F_i(\mathbf{x}_{t-1,\kappa}^{(i)}) + \bar{K} \nabla F(\tilde{\mathbf{x}}_{t-1}) \right\rangle
\end{aligned}$$

$$\begin{aligned}
& + \bar{K} \sum_{i, K_i \leq \bar{K}} \sum_{k=0}^{K_i-1} \frac{\omega_i}{\bar{K}_i} \left( \nabla F_i(\mathbf{x}_{t-1,k}^{(i)}) - \nabla F_i(\tilde{\mathbf{x}}_{t-1}) \right) \Bigg\} \text{and (a) follows triangle inequality, i.e., } (x+y)^2 \leq (1+c)x^2 + (1+1/c)y^2 \text{ for all } c > 0. \text{ We denote Equation (21)} \\
& - \eta(1-\lambda)K_{\max} \mathbb{E} \left\langle \nabla F(\tilde{\mathbf{x}}_t), \frac{1}{K_{\max}} \sum_{i=1}^M \sum_{k=0}^{K_i-1} \omega_i \nabla F_i(\mathbf{x}_{t,k}^{(i)}) \right\rangle \text{ omitted the coefficient } \frac{\eta\lambda}{2\bar{K}} \text{ by } T_2. \text{ Therefore, its upper bound} \\
& = -\frac{\eta\lambda\bar{K}}{2} \|\nabla F(\tilde{\mathbf{x}}_t)\|_2^2 \quad (19) \quad T_2 \stackrel{(a)}{\leq} 5\bar{K}^2 \mathbb{E} \|\nabla F(\tilde{\mathbf{x}}_t) - \nabla F(\tilde{\mathbf{x}}_{t-1})\|_2^2 \\
& - \frac{\eta\lambda}{2\bar{K}} \mathbb{E} \left\| \sum_{i=1}^M \sum_{k=0}^{K_i-1} \omega_i \nabla F_i(\mathbf{x}_{t,k}^{(i)}) \right. \\
& \quad \left. - \sum_{i=1}^M \sum_{\kappa=0}^{K_i-1} \omega_i \nabla F_i(\mathbf{x}_{t-1,\kappa}^{(i)}) + \bar{K} \nabla F(\tilde{\mathbf{x}}_{t-1}) \right. \\
& \quad \left. + \bar{K} \sum_{i, K_i \leq \bar{K}} \sum_{k=0}^{K_i-1} \frac{\omega_i}{\bar{K}_i} \left( \nabla F_i(\mathbf{x}_{t-1,k}^{(i)}) - \nabla F_i(\tilde{\mathbf{x}}_{t-1}) \right) \right\|_2^2 \\
& \quad + \frac{\eta\lambda}{2\bar{K}} \mathbb{E} \|\bar{K} \nabla F(\tilde{\mathbf{x}}_t) - \bar{K} \nabla F(\tilde{\mathbf{x}}_{t-1}) \\
& \quad - \sum_{i=1}^M \sum_{k=0}^{K_i-1} \omega_i \left( \nabla F_i(\mathbf{x}_{t,k}^{(i)}) - \nabla F_i(\mathbf{x}_{t-1,k}^{(i)}) \right) \\
& \quad - \bar{K} \sum_{i, K_i \leq \bar{K}} \sum_{k=0}^{K_i-1} \frac{\omega_i}{\bar{K}_i} \left( \nabla F_i(\mathbf{x}_{t-1,k}^{(i)}) - \nabla F_i(\tilde{\mathbf{x}}_{t-1}) \right) \Bigg\|_2^2 \quad (20) \\
& - \frac{\eta(1-\lambda)K_{\max}}{2} \mathbb{E} \|\nabla F(\tilde{\mathbf{x}}_t)\|_2^2 \quad (21) \\
& - \frac{\eta(1-\lambda)}{2K_{\max}} \mathbb{E} \left\| \sum_{i=1}^M \sum_{k=0}^{K_i-1} \omega_i \nabla F_i(\mathbf{x}_{t,k}^{(i)}) \right\|_2^2 \quad (22) \\
& + \frac{\eta(1-\lambda)K_{\max}}{2} \mathbb{E} \|\nabla F(\tilde{\mathbf{x}}_t) \\
& \quad - \frac{1}{K_{\max}} \sum_{i=1}^M \sum_{k=0}^{K_i-1} \omega_i \nabla F_i(\mathbf{x}_{t,k}^{(i)}) \Bigg\|_2^2 \quad (23) \\
& \quad - \frac{1}{K_{\max}} \sum_{i=1}^M \sum_{k=0}^{K_i-1} \omega_i \nabla F_i(\mathbf{x}_{t,k}^{(i)}) \Bigg\|_2^2 \quad (24)
\end{aligned}$$

Next, we bound the term of Equation (24) ignoring the coefficient term, i.e.,  $\frac{\eta(1-\lambda)K_{\max}}{2}$ :

$$\begin{aligned}
& \mathbb{E} \left\| \nabla F(\tilde{\mathbf{x}}_t) - \frac{1}{K_{\max}} \sum_{i=1}^M \sum_{k=0}^{K_i-1} \omega_i \nabla F_i(\mathbf{x}_{t,k}^{(i)}) \right\|_2^2 \\
& \leq \mathbb{E} \left\| \sum_{i=1}^M \omega_i \left( 1 - \frac{K_i}{K_{\max}} \right) \nabla F(\tilde{\mathbf{x}}_t) \right. \\
& \quad \left. - \frac{1}{K_{\max}} \sum_{i=1}^M \sum_{k=0}^{K_i-1} \omega_i \left( \nabla F_i(\tilde{\mathbf{x}}_t) - \nabla F_i(\mathbf{x}_{t,k}^{(i)}) \right) \right\|_2^2 \\
& \stackrel{(a)}{\leq} \left( 1 + \frac{K_{\min}}{K_{\max}} \right) \mathbb{E} \left\| \sum_{i=1}^M \omega_i \left( 1 - \frac{K_i}{K_{\max}} \right) \nabla F_i(\tilde{\mathbf{x}}_t) \right\|_2^2 \\
& \quad + \left( 1 + \frac{K_{\max}}{K_{\min}} \right) T_1 \\
& \leq \left( 1 - \frac{\bar{K}}{K_{\max}} \right) B^2 \mathbb{E} \|\nabla F(\tilde{\mathbf{x}}_t)\|_2^2 + \left( 1 + \frac{K_{\max}}{K_{\min}} \right) T_1
\end{aligned}$$

where

$$\begin{aligned}
T_1 & = \mathbb{E} \left\| \frac{1}{K_{\max}} \sum_{i=1}^M \sum_{k=0}^{K_i-1} \omega_i \left( \nabla F_i(\tilde{\mathbf{x}}_t) - \nabla F_i(\mathbf{x}_{t,k}^{(i)}) \right) \right\|_2^2 \\
& \leq \frac{L^2}{K_{\max}^2} \sum_{i=1}^M \sum_{k=0}^{K_i-1} \omega_i K_i \mathbb{E} \|\mathbf{x}_{t,k}^{(i)} - \tilde{\mathbf{x}}_t\|_2^2
\end{aligned}$$

$$\begin{aligned}
& \leq 5L^2 \left( \bar{K}^2 + \sum_{i=1}^M \omega_i K_i^2 \right) \mathbb{E} \|\tilde{\mathbf{x}}_t - \tilde{\mathbf{x}}_{t-1}\|_2^2 \\
& \quad + 5L^2 \sum_{i=1}^M \sum_{k=0}^{K_i-1} \omega_i K_i \mathbb{E} \|\mathbf{x}_{t,k}^{(i)} - \tilde{\mathbf{x}}_t\|_2^2 \\
& \quad + 5L^2 \sum_{i=1}^M \sum_{k=0}^{K_i-1} \omega_i K_i \mathbb{E} \|\mathbf{x}_{t-1,k}^{(i)} - \tilde{\mathbf{x}}_{t-1}\|_2^2 \\
& \quad + 5\bar{K}^2 L^2 \sum_{i, K_i \leq \bar{K}} \sum_{k=0}^{K_i-1} \frac{\omega_i}{\bar{K}_i} \mathbb{E} \|\mathbf{x}_{t-1,k}^{(i)} - \tilde{\mathbf{x}}_{t-1}\|_2^2 \\
& \leq 10L^2 \sum_{i=1}^M \omega_i K_i^2 \mathbb{E} \|\tilde{\mathbf{x}}_t - \tilde{\mathbf{x}}_{t-1}\|_2^2 \\
& \quad + 5L^2 \sum_{i=1}^M \sum_{k=0}^{K_i-1} \omega_i K_i \mathbb{E} \|\mathbf{x}_{t,k}^{(i)} - \tilde{\mathbf{x}}_t\|_2^2 \\
& \quad + 5L^2 \sum_{i=1}^M \sum_{k=0}^{K_i-1} \omega_i \left( K_i + \frac{\bar{K}^2}{K_i} \right) \mathbb{E} \|\mathbf{x}_{t-1,k}^{(i)} - \tilde{\mathbf{x}}_{t-1}\|_2^2 \quad (25)
\end{aligned}$$

where (a) divides  $(\nabla F_i(\mathbf{x}_{t,k}^{(i)}) - \nabla F_i(\mathbf{x}_{t-1,k}^{(i)}))$  into three terms, i.e., (each bracket should be treated as an individual term):  $(\nabla F_i(\mathbf{x}_{t,k}^{(i)}) - \nabla F_i(\tilde{\mathbf{x}}_t)) - (\nabla F_i(\mathbf{x}_{t-1,k}^{(i)}) - \nabla F_i(\tilde{\mathbf{x}}_{t-1})) + (\nabla F_i(\tilde{\mathbf{x}}_t) - \nabla F_i(\tilde{\mathbf{x}}_{t-1}))$ . By observing Equation (25), we notice that it is indispensable to acquire the upper limit of  $\mathbb{E} \|\mathbf{x}_{t,k}^{(i)} - \tilde{\mathbf{x}}_t\|_2^2$ :

$$\begin{aligned}
& \mathbb{E} \|\mathbf{x}_{t,k}^{(i)} - \tilde{\mathbf{x}}_t\|_2^2 \\
& = \mathbb{E} \|\mathbf{x}_{t,k-1}^{(i)} - \eta [g_{t,k-1}^{(i)} + \lambda(\nu - \nu^{(i)})] - \tilde{\mathbf{x}}_t\|_2^2 \\
& \leq \left( 1 + \frac{1}{K_i - 1} \right) \mathbb{E} \|\mathbf{x}_{t,k-1}^{(i)} - \tilde{\mathbf{x}}_t\|_2^2 \\
& \quad + K_i \eta^2 \mathbb{E} \left\| g_{t,k-1}^{(i)} - \frac{\lambda}{K_i} \sum_{\kappa=0}^{K_i-1} g_{t-1,\kappa}^{(i)} + \lambda \sum_{j=1}^M \sum_{k=0}^{K_j-1} \frac{\omega_j}{K_j} g_{t-1,k}^{(j)} \right. \\
& \quad \left. + \lambda \sum_{j, K_j > \bar{K}} \sum_{k=0}^{K_j-1} \frac{\omega_j}{K_j} (g_{t-1,0}^{(j)} - g_{t-1,k}^{(j)}) \right\|_2^2 \\
& \leq \left( 1 + \frac{1}{K_i - 1} \right) \mathbb{E} \|\mathbf{x}_{t,k-1}^{(i)} - \tilde{\mathbf{x}}_t\|_2^2 \quad (26)
\end{aligned}$$

$$\begin{aligned}
& + K_i \eta^2 \mathbb{E} \left\| \nabla F_i(\mathbf{x}_{t,k-1}^{(i)}) - \frac{\lambda}{K_i} \sum_{\kappa=0}^{K_i-1} \nabla F_i(\mathbf{x}_{t-1,\kappa}^{(i)}) \right. \\
& \quad + \lambda \sum_{j=1}^M \frac{\omega_j}{K_j} \sum_{k=0}^{K_j-1} \nabla F_j(\mathbf{x}_{t-1,k}^{(j)}) \\
& \quad \left. + \lambda \sum_{j, K_j > \bar{K}} \frac{\omega_j}{K_j} \sum_{k=0}^{K_j-1} \left( \nabla F_j(\tilde{\mathbf{x}}_{t-1}) - \nabla F_j(\mathbf{x}_{t-1,k}^{(j)}) \right) \right\|_2^2 \\
& + 4K_i^2 \eta^2 \sigma^2 + 4\lambda^2 \eta^2 \sigma^2 + 12K_i^2 \eta^2 \lambda^2 \sigma^2 \sum_{j=1}^M \frac{\omega_j^2}{K_j} \quad (28)
\end{aligned}$$

We denote the second norm in Equation (27) by  $T_3$ . Similar to the derivation for  $T_2$ , i.e., Equation (25), we have the following inequality under Assumption 4:

$$\begin{aligned}
T_3 & \leq 8L^2 \mathbb{E} \left\| \mathbf{x}_{t,k-1}^{(i)} - \tilde{\mathbf{x}}_t \right\|_2^2 + \frac{8\lambda^2 L^2}{K_i} \sum_{\kappa=0}^{K_i-1} \mathbb{E} \left\| \mathbf{x}_{t-1,\kappa}^{(i)} - \tilde{\mathbf{x}}_{t-1} \right\|_2^2 \\
& + 16\lambda^2 L^2 \sum_{j=1}^M \sum_{k=0}^{K_j-1} \frac{\omega_j}{K_j} \mathbb{E} \left\| \mathbf{x}_{t-1,k}^{(j)} - \tilde{\mathbf{x}}_{t-1} \right\|_2^2 \\
& + 8((1-\lambda)^2 B^2 + \lambda^2) \mathbb{E} \left\| \nabla F(\tilde{\mathbf{x}}_t) \right\|_2^2 \\
& + 16\lambda^2 L^2 \mathbb{E} \left\| \tilde{\mathbf{x}}_t - \tilde{\mathbf{x}}_{t-1} \right\|_2^2 \quad (29)
\end{aligned}$$

By setting  $\eta \leq \frac{1}{2\sqrt{2}LK_{\max}}$  and following the steps of Equation (17), we have:

$$\mathbb{E} \left\| \mathbf{x}_{t,k}^{(i)} - \tilde{\mathbf{x}}_t \right\|_2^2 \leq \frac{K_i - 1}{2} \left( \left( 1 + \frac{2}{K_i - 1} \right)^{k+1} - 1 \right) T_4 \quad (30)$$

where

$$\begin{aligned}
T_4 & = 16\lambda^2 L^2 K_i \eta^2 \left\| \tilde{\mathbf{x}}_t - \tilde{\mathbf{x}}_{t-1} \right\|_2^2 \\
& + 8\lambda^2 L^2 \eta^2 \sum_{k=0}^{K_i-1} \left\| \mathbf{x}_{t-1,k}^{(i)} - \tilde{\mathbf{x}}_{t-1} \right\|_2^2 \\
& + 16\lambda^2 L^2 K_i \eta^2 \sum_{j=1}^M \sum_{k=0}^{K_j-1} \frac{\omega_j}{K_j} \left\| \mathbf{x}_{t-1,k}^{(j)} - \tilde{\mathbf{x}}_{t-1} \right\|_2^2 \\
& + 8K_i \eta^2 ((1-\lambda)^2 B^2 + \lambda^2) \left\| \nabla F(\tilde{\mathbf{x}}_t) \right\|_2^2 + 4K_i \eta^2 \sigma^2 \\
& + 4\lambda^2 \eta^2 \sigma^2 + 12K_i \eta^2 \lambda^2 \sigma^2 \sum_{j=1}^M \frac{\omega_j^2}{K_j}.
\end{aligned}$$

As a result, when the learning rate  $\eta$  is sufficiently small, the upper bound for  $T_2$  should be

$$\begin{aligned}
T_2 & \leq \left( 20L^2 \sum_{i=1}^M \omega_i K_i^2 \right) \mathbb{E} \left\| \tilde{\mathbf{x}}_t - \tilde{\mathbf{x}}_{t-1} \right\|_2^2 \\
& + 20\bar{K}^2 L^2 \sum_{i=1}^M \sum_{k=0}^{K_i-1} \omega_i \mathbb{E} \left\| \mathbf{x}_{t-1,k}^{(i)} - \tilde{\mathbf{x}}_{t-1} \right\|_2^2 \\
& + 60\eta^2 L^2 K_{\max}^4 ((1-\lambda)^2 B^2 + \lambda^2) \mathbb{E} \left\| \nabla F(\tilde{\mathbf{x}}_t) \right\|_2^2 \\
& + 30\eta^2 L^2 \sigma^2 \sum_{i=1}^M \omega_i K_i^4 + 30\eta^2 L^2 \sigma^2 \lambda^2 \sum_{i=1}^M \omega_i K_i^3 \\
& + 90\eta^2 L^2 \sigma^2 \lambda^2 \left( \sum_{j=1}^M \frac{\omega_j^2}{K_j} \right) \sum_{i=1}^M \omega_i K_i^4 \quad (31)
\end{aligned}$$

**The second term of Equation (18).** We now give the upper limit for  $\mathbb{E} \left\| \tilde{\mathbf{x}}_{t+1} - \tilde{\mathbf{x}}_t \right\|_2^2$ :

$$\begin{aligned}
& \mathbb{E} \left\| \tilde{\mathbf{x}}_{t+1} - \tilde{\mathbf{x}}_t \right\|_2^2 \\
& \leq \eta^2 \mathbb{E} \left\| \sum_{i=1}^M \sum_{k=0}^{K_i-1} \omega_i \nabla F_i(\mathbf{x}_{t,k}^{(i)}) \right. \\
& \quad + \lambda \sum_{i, K_i > \bar{K}} \sum_{k=0}^{K_i-1} \frac{\omega_i \bar{K}}{K_i} \left( \nabla F_i(\tilde{\mathbf{x}}_{t-1}) - \nabla F_i(\mathbf{x}_{t-1,k}^{(i)}) \right) \\
& \quad \left. + \lambda \sum_{i=1}^M \sum_{k=0}^{K_i-1} \omega_i \left( \frac{\bar{K}}{K_i} - 1 \right) \nabla F_i(\mathbf{x}_{t-1,k}^{(i)}) \right\|_2^2 \\
& \leq 2\eta^2 \lambda^2 \mathbb{E} \left\| \sum_{i=1}^M \sum_{k=0}^{K_i-1} \omega_i \nabla F_i(\mathbf{x}_{t,k}^{(i)}) - \sum_{i=1}^M \sum_{\kappa=0}^{K_i-1} \omega_i \nabla F_i(\mathbf{x}_{t-1,\kappa}^{(i)}) \right. \\
& \quad + \sum_{i, K_i \leq \bar{K}} \frac{\omega_i \bar{K}}{K_i} \sum_{k=0}^{K_i-1} \left( \nabla F_i(\mathbf{x}_{t-1,k}^{(i)}) - \nabla F_i(\tilde{\mathbf{x}}_{t-1}) \right) \\
& \quad \left. + \bar{K} \nabla F(\tilde{\mathbf{x}}_{t-1}) \right\|_2^2 \\
& + 2\eta^2 (1-\lambda)^2 \left\| \sum_{i=1}^M \sum_{k=0}^{K_i-1} \omega_i \nabla F_i(\mathbf{x}_{t,k}^{(i)}) \right\|_2^2 \\
& + 3\eta^2 \sigma^2 \sum_{i=1}^M \omega_i^2 K_i + 3\eta^2 \lambda^2 \sigma^2 \sum_{i=1}^M \omega_i^2 \left( \frac{5\bar{K}^2}{K_i} + K_i \right) \quad (32)
\end{aligned}$$

**Final result.** By the inequality from Equation (31) and Equation (32), we can add two extra terms on the left-hand side of Equation (18), i.e.,  $\mathbb{E} \left\| \tilde{\mathbf{x}}_t - \tilde{\mathbf{x}}_{t-1} \right\|_2^2$  and  $\sum_{i=1}^M \sum_{k=0}^{K_i-1} \omega_i K_i \mathbb{E} \left\| \mathbf{x}_{t-1,k}^{(i)} - \tilde{\mathbf{x}}_{t-1} \right\|_2^2$ , and obtain the following bound when the learning rate is sufficiently small:

$$\begin{aligned}
& \mathbb{E}[F(\tilde{\mathbf{x}}_{t+1})] + p_1 \mathbb{E} \left\| \tilde{\mathbf{x}}_{t+1} - \tilde{\mathbf{x}}_t \right\|_2^2 + p_2 \sum_{i=1}^M \sum_{k=0}^{K_i-1} \omega_i K_i \mathbb{E} \left\| \mathbf{x}_{t,k}^{(i)} - \tilde{\mathbf{x}}_t \right\|_2^2 \\
& \leq F(\tilde{\mathbf{x}}_t) + p_1 \mathbb{E} \left\| \tilde{\mathbf{x}}_t - \tilde{\mathbf{x}}_{t-1} \right\|_2^2 + p_2 \sum_{i=1}^M \sum_{k=0}^{K_i-1} \omega_i K_i \mathbb{E} \left\| \mathbf{x}_{t-1,k}^{(i)} - \tilde{\mathbf{x}}_{t-1} \right\|_2^2 \\
& \quad - \left( \frac{\eta \lambda \bar{K}}{2} + \frac{\eta(1-\lambda) K_{\max}}{2} \left( 1 - \left( 1 - \frac{\bar{K}}{K_{\max}} \right) B^2 \right) \right) \left\| \nabla F(\tilde{\mathbf{x}}_t) \right\|_2^2 \\
& \quad + 3 \left( \frac{L}{2} + p_1 \right) \eta^2 \sigma^2 \left( \sum_{i=1}^M \omega_i^2 K_i + \lambda^2 \sum_{i=1}^M \omega_i^2 \left( \frac{5\bar{K}^2}{K_i} + K_i \right) \right)
\end{aligned}$$

where  $p_1 = o\left(\frac{\eta \lambda}{\bar{K}} L^2 \sum_{i=1}^M \omega_i (K_i^2 + \bar{K}^2)\right)$  and  $p_2 = o\left(\frac{\eta \lambda}{\bar{K}} L^2 \left(1 + \frac{\bar{K}^2}{K_{\min}^2}\right)\right)$ . Therefore, the final result is:

$$\begin{aligned}
& \frac{1}{T} \sum_{t=1}^T \left\| \nabla F(\tilde{\mathbf{x}}_t) \right\|_2^2 \\
& = \mathcal{O} \left( \frac{F(\mathbf{x}_*) - F(\tilde{\mathbf{x}}_1)}{\eta \lambda \bar{K} T} \right) + \mathcal{O} \left( \frac{\eta \sigma^2 L}{\lambda \bar{K}} \sum_{i=1}^M \omega_i^2 K_i \right) \\
& \quad + \mathcal{O} \left( \frac{\eta \sigma^2 L \lambda}{\bar{K}} \sum_{i=1}^M \omega_i^2 \left( \frac{\bar{K}}{K_i} - 1 \right)^2 \right) + \mathcal{O} \left( \eta \sigma^2 L \lambda \sum_{i, K_i > \bar{K}} \frac{\omega_i^2 \bar{K}}{K_i} \right)
\end{aligned}$$

## APPENDIX C PROOF OF THEOREM 3

At the very beginning, we set  $\lambda = 1$  to find a valid bound. Based on the definition, we can find a recursion function for

$$\mathbb{E} \|\tilde{\mathbf{x}}_{t+1} - \mathbf{x}_*\|_2^2:$$

$$\begin{aligned} \mathbb{E} \|\tilde{\mathbf{x}}_{t+1} - \mathbf{x}_*\|_2^2 &= \mathbb{E} \|(\tilde{\mathbf{x}}_t - \mathbf{x}_*) + (\tilde{\mathbf{x}}_{t+1} - \tilde{\mathbf{x}}_t)\|_2^2 \\ &= \mathbb{E} \|\tilde{\mathbf{x}}_t - \mathbf{x}_*\|_2^2 + \mathbb{E} \|\tilde{\mathbf{x}}_{t+1} - \tilde{\mathbf{x}}_t\|_2^2 + 2\mathbb{E} \langle \tilde{\mathbf{x}}_t - \mathbf{x}_*, \tilde{\mathbf{x}}_{t+1} - \tilde{\mathbf{x}}_t \rangle \\ &= \mathbb{E} \|\tilde{\mathbf{x}}_t - \mathbf{x}_*\|_2^2 + \mathbb{E} \|\tilde{\mathbf{x}}_{t+1} - \tilde{\mathbf{x}}_t\|_2^2 \end{aligned} \quad (33)$$

$$+ 2\mathbb{E} \left\langle \tilde{\mathbf{x}}_t - \mathbf{x}_*, -\eta \sum_{i=1}^M \sum_{k=0}^{K_i-1} \omega_i \nabla F_i(\mathbf{x}_{t,k}^{(i)}) \right\rangle \quad (34)$$

$$+ 2\mathbb{E} \left\langle \tilde{\mathbf{x}}_t - \mathbf{x}_*, \eta \sum_{i=1}^M \sum_{k=0}^{K_i-1} \omega_i \nabla F_i(\mathbf{x}_{t-1,k}^{(i)}) \right\rangle \quad (35)$$

$$+ 2\mathbb{E} \langle \tilde{\mathbf{x}}_t - \mathbf{x}_*, -\eta \bar{K} \sum_{i, K_i \leq \bar{K}} \frac{\omega_i}{K_i} \sum_{k=0}^{K_i-1} (\nabla F_i(\mathbf{x}_{t-1,k}^{(i)}) - \nabla F_i(\tilde{\mathbf{x}}_{t-1})) \rangle \quad (36)$$

$$+ 2\mathbb{E} \langle \tilde{\mathbf{x}}_t - \mathbf{x}_*, -\eta \bar{K} \nabla F(\tilde{\mathbf{x}}_{t-1}) \rangle \quad (37)$$

We denote Equation (34) to (37) by  $\mathcal{Q}_1$ ,  $\mathcal{Q}_2$ ,  $\mathcal{Q}_3$  and  $\mathcal{Q}_4$ , respectively. There are two terms in Equation (34) and Equation (35), namely  $\mathcal{Q}_1$  and  $\mathcal{Q}_2$ , between which the subscript is different (i.e., one for  $t$ -th update while the others for  $t-1$ -th update). The following will present how to bound  $\mathcal{Q}_1$  first, and then  $\mathcal{Q}_2$ .

$$\begin{aligned} \mathcal{Q}_1 &= \eta \sum_{i=1}^M \sum_{k=0}^{K_i-1} \omega_i \mathbb{E} \langle \nabla F_i(\mathbf{x}_{t,k}^{(i)}) - \nabla F_i(\tilde{\mathbf{x}}_t), \mathbf{x}_* - \tilde{\mathbf{x}}_t \rangle \\ &\quad + \eta \sum_{i=1}^M \omega_i K_i \mathbb{E} \langle \nabla F_i(\tilde{\mathbf{x}}_t), \mathbf{x}_* - \tilde{\mathbf{x}}_t \rangle \\ &\leq \frac{\eta}{2} \sum_{i=1}^M \sum_{k=0}^{K_i-1} \omega_i \left( \frac{16}{\mu} \mathbb{E} \|\nabla F_i(\mathbf{x}_{t,k}^{(i)}) - \nabla F_i(\tilde{\mathbf{x}}_t)\|_2^2 \right. \\ &\quad \left. + \frac{\mu}{16} \mathbb{E} \|\mathbf{x}_* - \tilde{\mathbf{x}}_t\|_2^2 \right) \\ &\quad + \eta \sum_{i=1}^M \omega_i K_i \mathbb{E} \langle \nabla F_i(\tilde{\mathbf{x}}_t), \mathbf{x}_* - \tilde{\mathbf{x}}_t \rangle \\ &\leq \frac{8\eta L^2}{\mu} \sum_{i=1}^M \sum_{k=0}^{K_i-1} \omega_i \mathbb{E} \|\mathbf{x}_{t,k}^{(i)} - \mathbf{x}_*\|_2^2 + \frac{\eta \mu \bar{K}}{32} \mathbb{E} \|\mathbf{x}_* - \tilde{\mathbf{x}}_t\|_2^2 \\ &\quad + \eta \sum_{i=1}^M \omega_i K_i \mathbb{E} \langle \nabla F_i(\tilde{\mathbf{x}}_t), \mathbf{x}_* - \tilde{\mathbf{x}}_t \rangle \end{aligned}$$

where the first inequality refers to  $\langle a, b \rangle \leq (\|a\|_2^2 + \|b\|_2^2)/2$  and the last one is according to Assumption 1. Likewise, we can find the bound for  $\mathcal{Q}_2$ :

$$\begin{aligned} \mathcal{Q}_2 &\leq \frac{8\eta L^2}{\mu} \sum_{i=1}^M \sum_{k=0}^{K_i-1} \omega_i \mathbb{E} \|\mathbf{x}_{t-1,k}^{(i)} - \mathbf{x}_*\|_2^2 \\ &\quad + \frac{\eta \mu \bar{K}}{32} \mathbb{E} \|\mathbf{x}_* - \tilde{\mathbf{x}}_t\|_2^2 \\ &\quad + \eta \sum_{i=1}^M \omega_i K_i \mathbb{E} \langle \nabla F_i(\tilde{\mathbf{x}}_{t-1}), \tilde{\mathbf{x}}_t - \mathbf{x}_* \rangle \end{aligned}$$

As a result, we have:

$$\mathcal{Q}_1 + \mathcal{Q}_2$$

$$\begin{aligned} &\leq \frac{8\eta L^2}{\mu} \sum_{i=1}^M \sum_{k=0}^{K_i-1} \omega_i \left( \mathbb{E} \|\mathbf{x}_{t,k}^{(i)} - \mathbf{x}_*\|_2^2 + \mathbb{E} \|\mathbf{x}_{t-1,k}^{(i)} - \mathbf{x}_*\|_2^2 \right) \\ &\quad + \eta \sum_{i=1}^M \omega_i K_i \mathbb{E} \langle \nabla F_i(\tilde{\mathbf{x}}_{t-1}) - \nabla F_i(\tilde{\mathbf{x}}_t), \tilde{\mathbf{x}}_t - \mathbf{x}_* \rangle \\ &\quad + \frac{\eta \mu \bar{K}}{16} \mathbb{E} \|\mathbf{x}_* - \tilde{\mathbf{x}}_t\|_2^2 \\ &\leq \frac{8\eta L^2}{\mu} \sum_{i=1}^M \sum_{k=0}^{K_i-1} \omega_i \left( \mathbb{E} \|\mathbf{x}_{t,k}^{(i)} - \mathbf{x}_*\|_2^2 + \mathbb{E} \|\mathbf{x}_{t-1,k}^{(i)} - \mathbf{x}_*\|_2^2 \right) \\ &\quad + \frac{3\eta \mu \bar{K}}{32} \mathbb{E} \|\mathbf{x}_* - \tilde{\mathbf{x}}_t\|_2^2 + \frac{8\eta \bar{K} L^2}{\mu} \mathbb{E} \|\tilde{\mathbf{x}}_t - \tilde{\mathbf{x}}_{t-1}\|_2^2 \end{aligned}$$

where the last inequality is based on  $\langle a, b \rangle \leq (\|a\|_2^2 + \|b\|_2^2)/2$  and Assumption 1.

For the term in Equation (36), according to the inequality that  $\langle a, b \rangle \leq (\|a\|_2^2 + \|b\|_2^2)/2$  and the assumption of L-smooth, we have:

$$\begin{aligned} \mathcal{Q}_3 &= -\eta \bar{K} \sum_{i, K_i \leq \bar{K}} \frac{\omega_i}{K_i} \sum_{k=0}^{K_i-1} \mathbb{E} \langle \tilde{\mathbf{x}}_t - \mathbf{x}_*, \\ &\quad \nabla F_i(\mathbf{x}_{t-1,k}^{(i)}) - \nabla F_i(\tilde{\mathbf{x}}_{t-1}) \rangle \\ &\leq \frac{8\eta \bar{K} L^2}{\mu} \sum_{i, K_i \leq \bar{K}} \sum_{k=0}^{K_i-1} \frac{\omega_i}{K_i} \mathbb{E} \|\mathbf{x}_{t-1,k}^{(i)} - \tilde{\mathbf{x}}_{t-1}\|_2^2 \\ &\quad + \frac{\eta \mu \bar{K}}{32} \mathbb{E} \|\mathbf{x}_* - \tilde{\mathbf{x}}_t\|_2^2 \end{aligned}$$

The last equality holds because  $\omega_i > 0$  and  $K_i > 0$  such that the sum for those  $K_i \leq \bar{K}$  is not greater than the one for all workers.

Based on Lemma 1 above, it is easy to derive the bound for  $\mathcal{Q}_4$ , which is:

$$\begin{aligned} \mathcal{Q}_4 &= \eta \bar{K} \mathbb{E} \langle \nabla F(\tilde{\mathbf{x}}_{t-1}), \mathbf{x}_* - \tilde{\mathbf{x}}_t \rangle \\ &\leq \eta \bar{K} \left( F(\mathbf{x}_*) - F(\tilde{\mathbf{x}}_t) - \frac{\mu}{4} \mathbb{E} \|\tilde{\mathbf{x}}_t - \mathbf{x}_*\|_2^2 + L \mathbb{E} \|\tilde{\mathbf{x}}_t - \tilde{\mathbf{x}}_{t-1}\|_2^2 \right) \end{aligned}$$

According to the bound for  $\mathbb{E} \|\tilde{\mathbf{x}}_{t+1} - \tilde{\mathbf{x}}_t\|_2^2$  in the proof non-convex objectives, i.e.,  $T_2$ , we have:

$$\begin{aligned} \mathbb{E} \|\tilde{\mathbf{x}}_{t+1} - \tilde{\mathbf{x}}_t\|_2^2 &\leq 2\eta^2 \lambda^2 \mathcal{Q}_5 + 3\eta^2 \sigma^2 \sum_{i=1}^M \omega_i^2 K_i \\ &\quad + 3\eta^2 \lambda^2 \sigma^2 \sum_{i=1}^M \omega_i^2 \left( \frac{\bar{K}}{K_i} - 1 \right)^2 K_i \\ &\quad + 12\eta^2 \lambda^2 \sigma^2 \sum_{i, K_i > \bar{K}} \frac{\omega_i^2 \bar{K}^2}{K_i} \end{aligned}$$

where

$$\begin{aligned} \mathcal{Q}_5 &= \mathbb{E} \left\| \sum_{i=1}^M \sum_{k=0}^{K_i-1} \omega_i \nabla F_i(\mathbf{x}_{t,k}^{(i)}) - \sum_{i=1}^M \sum_{k=0}^{K_i-1} \omega_i \nabla F_i(\mathbf{x}_{t-1,k}^{(i)}) \right. \\ &\quad \left. + \bar{K} \sum_{i, K_i \leq \bar{K}} \frac{\omega_i}{K_i} \sum_{k=0}^{K_i-1} (\nabla F_i(\mathbf{x}_{t-1,k}^{(i)}) - \nabla F_i(\tilde{\mathbf{x}}_{t-1})) \right. \\ &\quad \left. + \bar{K} \nabla F(\tilde{\mathbf{x}}_{t-1}) \right\|_2^2 \end{aligned} \quad (38)$$



Unlike the procedure in non-convex objectives,  $\mathcal{Q}_5$  cannot be eliminated. Therefore, we should find a general bound for Equation (36), where we can further simplify as:

$$\begin{aligned}
\mathcal{Q}_5 &= \mathbb{E} \left\| \sum_{i=1}^M \sum_{k=0}^{K_i-1} \omega_i \left( \nabla F_i \left( \mathbf{x}_{t,k}^{(i)} \right) - \nabla F_i \left( \tilde{\mathbf{x}}_t \right) \right) \right. \\
&\quad - \sum_{i=1}^M \sum_{k=0}^{K_i-1} \omega_i \left( \nabla F_i \left( \mathbf{x}_{t-1,k}^{(i)} \right) - \nabla F_i \left( \tilde{\mathbf{x}}_{t-1} \right) \right) \\
&\quad + \bar{K} \sum_{i, K_i \leq \bar{K}} \frac{\omega_i}{K_i} \sum_{k=0}^{K_i-1} \left( \nabla F_i \left( \mathbf{x}_{t-1,k}^{(i)} \right) - \nabla F_i \left( \tilde{\mathbf{x}}_{t-1} \right) \right) \\
&\quad + \bar{K} \left( \nabla F \left( \tilde{\mathbf{x}}_{t-1} \right) - \nabla F \left( \tilde{\mathbf{x}}_t \right) \right) + \bar{K} \nabla F \left( \tilde{\mathbf{x}}_t \right) \\
&\quad \left. + \sum_{i=1}^M \omega_i K_i \left( \nabla F_i \left( \tilde{\mathbf{x}}_t \right) - \nabla F_i \left( \tilde{\mathbf{x}}_{t-1} \right) \right) \right\|_2^2 \\
&\leq 6L^2 \sum_{i=1}^M \sum_{k=0}^{K_i-1} \omega_i K_i \mathbb{E} \left\| \mathbf{x}_{t,k}^{(i)} - \tilde{\mathbf{x}}_t \right\|_2^2 \\
&\quad + 6L^2 \sum_{i=1}^M \sum_{k=0}^{K_i-1} \omega_i K_i \mathbb{E} \left\| \mathbf{x}_{t-1,k}^{(i)} - \tilde{\mathbf{x}}_{t-1} \right\|_2^2 \\
&\quad + 6\bar{K}^2 L^2 \sum_{i, K_i \leq \bar{K}} \sum_{k=0}^{K_i-1} \frac{\omega_i}{K_i} \mathbb{E} \left\| \mathbf{x}_{t-1,k}^{(i)} - \tilde{\mathbf{x}}_{t-1} \right\|_2^2 \\
&\quad + 12\bar{K}^2 L^2 \mathbb{E} \left\| \tilde{\mathbf{x}}_t - \tilde{\mathbf{x}}_{t-1} \right\|_2^2 + 6\bar{K}^2 L^2 \mathbb{E} \left\| \tilde{\mathbf{x}}_t - \mathbf{x}_* \right\|_2^2
\end{aligned}$$

Plugging the results above, we can obtain the bound for  $\mathbb{E} \left\| \tilde{\mathbf{x}}_{t+1} - \mathbf{x}_* \right\|_2^2$  as:

$$\begin{aligned}
&\mathbb{E} \left\| \tilde{\mathbf{x}}_{t+1} - \mathbf{x}_* \right\|_2^2 \\
&\leq \left( 1 - \frac{\eta\mu\bar{K}}{4} \right) \mathbb{E} \left\| \tilde{\mathbf{x}}_t - \mathbf{x}_* \right\|_2^2 \\
&\quad + 12\eta^2 \lambda^2 L^2 \sum_{i=1}^M \sum_{k=0}^{K_i-1} \omega_i K_i \mathbb{E} \left\| \mathbf{x}_{t,k}^{(i)} - \tilde{\mathbf{x}}_t \right\|_2^2 \\
&\quad + 12\eta^2 \lambda^2 L^2 \sum_{i=1}^M \sum_{k=0}^{K_i-1} \omega_i K_i \mathbb{E} \left\| \mathbf{x}_{t-1,k}^{(i)} - \tilde{\mathbf{x}}_{t-1} \right\|_2^2 \\
&\quad + 12\eta^2 \lambda^2 \bar{K}^2 L^2 \sum_{i, K_i \leq \bar{K}} \sum_{k=0}^{K_i-1} \frac{\omega_i}{K_i} \mathbb{E} \left\| \mathbf{x}_{t-1,k}^{(i)} - \tilde{\mathbf{x}}_{t-1} \right\|_2^2 \\
&\quad + 24\eta^2 \lambda^2 \bar{K}^2 L^2 \mathbb{E} \left\| \tilde{\mathbf{x}}_t - \tilde{\mathbf{x}}_{t-1} \right\|_2^2 + 12\eta^2 \lambda^2 \bar{K}^2 L^2 \mathbb{E} \left\| \tilde{\mathbf{x}}_t - \mathbf{x}_* \right\|_2^2 \\
&\quad + 3\eta^2 \sigma^2 \sum_{i=1}^M \omega_i^2 K_i + 3\eta^2 \lambda^2 \sigma^2 \sum_{i=1}^M \omega_i^2 \left( \frac{\bar{K}}{K_i} - 1 \right)^2 K_i \\
&\quad + 12\eta^2 \lambda^2 \sigma^2 \sum_{i, K_i > \bar{K}} \frac{\omega_i^2 \bar{K}^2}{K_i} \\
&\quad + \frac{16\eta L^2}{\mu} \sum_{i=1}^M \sum_{k=0}^{K_i-1} \omega_i \left( \mathbb{E} \left\| \mathbf{x}_{t,k}^{(i)} - \mathbf{x}_* \right\|_2^2 + \mathbb{E} \left\| \mathbf{x}_{t-1,k}^{(i)} - \mathbf{x}_* \right\|_2^2 \right) \\
&\quad + \frac{16\eta \bar{K} L^2}{\mu} \mathbb{E} \left\| \tilde{\mathbf{x}}_t - \tilde{\mathbf{x}}_{t-1} \right\|_2^2 \\
&\quad + \frac{16\eta \bar{K} L^2}{\mu} \sum_{i, K_i \leq \bar{K}} \sum_{k=0}^{K_i-1} \frac{\omega_i}{K_i} \mathbb{E} \left\| \mathbf{x}_{t-1,k}^{(i)} - \tilde{\mathbf{x}}_{t-1} \right\|_2^2 \\
&\quad + 2\eta \bar{K} \left( F \left( \mathbf{x}_* \right) - F \left( \tilde{\mathbf{x}}_t \right) + L \mathbb{E} \left\| \tilde{\mathbf{x}}_t - \tilde{\mathbf{x}}_{t-1} \right\|_2^2 \right)
\end{aligned}$$

By observation, there are two recursive formulas, i.e.,  $\mathbb{E} \left\| \tilde{\mathbf{x}}_t - \tilde{\mathbf{x}}_{t-1} \right\|_2^2$  and  $\sum_{i=1}^M \sum_{k=0}^{K_i-1} \omega_i K_i \mathbb{E} \left\| \mathbf{x}_{t-1,k}^{(i)} - \tilde{\mathbf{x}}_{t-1} \right\|_2^2$ , and the coefficients of both of them contain the stepsize  $\eta$ . To release these formulas, we let the formula on the left-hand side be the formula as follows:

$$\begin{aligned}
\mathcal{Y}_{t+1} &= \mathbb{E} \left\| \tilde{\mathbf{x}}_{t+1} - \mathbf{x}_* \right\|_2^2 + u_1 \mathbb{E} \left\| \tilde{\mathbf{x}}_{t+1} - \tilde{\mathbf{x}}_t \right\|_2^2 \\
&\quad + u_2 \sum_{i=1}^M \sum_{k=0}^{K_i-1} \omega_i K_i \mathbb{E} \left\| \mathbf{x}_{t,k}^{(i)} - \tilde{\mathbf{x}}_t \right\|_2^2
\end{aligned}$$

where  $u_1$  and  $u_2$  are the coefficients containing the step-size of  $\eta$  such that the coefficient for  $\mathbb{E} \left\| \tilde{\mathbf{x}}_t - \tilde{\mathbf{x}}_{t-1} \right\|_2^2$  and  $\sum_{i=1}^M \sum_{k=0}^{K_i-1} \omega_i K_i \mathbb{E} \left\| \mathbf{x}_{t-1,k}^{(i)} - \tilde{\mathbf{x}}_{t-1} \right\|_2^2$  on the right hand side become negative and thereby, can be omitted when finding the bound. Also, we notice that the added term includes  $\eta^2$  after simplification. Therefore, the formula can be further simplified as:

$$\begin{aligned}
\mathcal{Y}_{t+1} &\leq \left( 1 - \frac{\eta\mu\bar{K}}{4} \right) \mathcal{Y}_t - 2\eta\bar{K} \left( F \left( \tilde{\mathbf{x}}_t \right) - F \left( \mathbf{x}_* \right) \right) \\
&\quad + 6\eta^2 \sigma^2 \sum_{i=1}^M \omega_i^2 K_i + 6\eta^2 \lambda^2 \sigma^2 \sum_{i=1}^M \omega_i^2 \left( \frac{\bar{K}}{K_i} - 1 \right)^2 K_i \\
&\quad + 24\eta^2 \lambda^2 \sigma^2 \sum_{i, K_i > \bar{K}} \frac{\omega_i^2 \bar{K}^2}{K_i}
\end{aligned}$$

The rest step is similar to the proof in Theorem 1. Therefore, we can obtain the expected result in Theorem 3. Different from Theorem 1, this theorem release the term of data heterogeneity and therefore, our result can successfully converge to the global optimizer.